#### Review article

Guang Liang Ong, Teng Sian Ong, Seong Ling Yap, Der-Jang Liaw, Teck Yong Tou, Seong Shan Yap, and Chen Hon Nee\*

# A brief review of nanoparticles-doped PEDOT:PSS nanocomposite for OLED and OPV

https://doi.org/10.1515/ntrev-2022-0104 received December 31, 2021; accepted March 19, 2022

**Abstract:** In recent years, several strategies have been proposed and demonstrated to enhance the efficiency of organic light-emitting diodes (OLEDs) and organic photovoltaics (OPVs). In both types of devices, poly(3,4-ethylenedioxythiophene):poly(styrene sulfonate) (PEDOT:PSS) is commonly used to enhance hole injection. The layer is further designed by incorporating metallic-based, carbonbased, organic, inorganic, and hybrid nanoparticles with the aim of improving the performance and hence the efficiency through the improvement of light out-coupling in OLEDs and enhancement in light absorption generation of hole-charge carriers in OPVs. This review elucidates the use of different types of nanoparticles that are doped into PEDOT:PSS and their effects on OLEDs or OPVs. The effects include surface plasmon resonance (SPR), scattering, better charge transport, improvement in surface morphology and electrical properties of PEDOT:PSS. Promising results have been obtained and can potentially lead to low cost, large-area manufacturing process.

**Keywords:** OLED, OPV, nanoparticles, PEDOT:PSS, organic electronics, surface plasmon resonance

e-mail: chnee@mmu.edu.my

Guang Liang Ong, Teng Sian Ong, Teck Yong Tou, Seong Shan Yap: Faculty of Engineering, Multimedia University, 63100 Cyberjaya, Malavsia

Seong Ling Yap: Plasma Research Laboratory, Department of Physics, Faculty of Science, University of Malaya, 50603 Kuala Lumpur, Malaysia

**Der-Jang Liaw:** Department of Chemical Engineering, National Taiwan University of Science and Technology, 10607 Taipei, Taiwan

## 1 Introduction

Organic optoelectronic devices, particularly organic lightemitting diodes (OLED) and organic photovoltaic (OPV) solar cells, have attracted attention in recent decades due to various advantages such as low cost, thinness, lightness, semi-transparency, and ability to be fabricated onto flexible substrates [1–6]. However, the efficiencies and long-term stability need to be improved. The improvement strategies include the use of new active layer materials [7–10], new functional layer materials (hole transport layer – HTL or electron transport layer – ETL) [3,11], doping of nanoparticles [12,13], and optimising the device structure [14].

In OLEDs, the injection of charge carriers from the contacting electrodes are required for emitting light. Holes are injected from the anode, and electrons are injected from top metallic cathode; hole-electron pairs are then recombined at the emissive layer where emission occurs [15]. OPVs work in the opposite way where light is absorbed, for example, in bulk heterojunction (BHJ), which consists of the blend of two semiconductors, a donor, and an acceptor. Due to the opposite charges of the hole and electron, they are attracted together to form electron-hole pair known as exciton. The electron-hole pair then separated into cathode and anode in a process known as exciton dissociation. In order to generate electric current, the photons must be continuously absorbed and converted into free charge carriers (electrons and holes) effectively [15].

The optical loss for OLEDs is about 80%, where most of the emitted light is trapped inside the OLED devices, and only the remaining ~20% is able to be extracted out of the substrate [16], as shown in Figure 1. Therefore, various approaches have been investigated to improve optical loss, including the use of silica microspheres [17], microlens arrays [18], and photonic crystal structure [19] for OLEDs. Another promising approach is by applying nano-structures into OLEDs as a scattering layer using nanoparticles (NPs) [20,21]. Compared to the other methods,

<sup>\*</sup> Corresponding author: Chen Hon Nee, Faculty of Engineering, Multimedia University, 63100 Cyberjaya, Malaysia,

**<sup>∂</sup>** Open Access. © 2022 Guang Liang Ong *et al.*, published by De Gruyter. This work is licensed under the Creative Commons Attribution 4.0 International License.

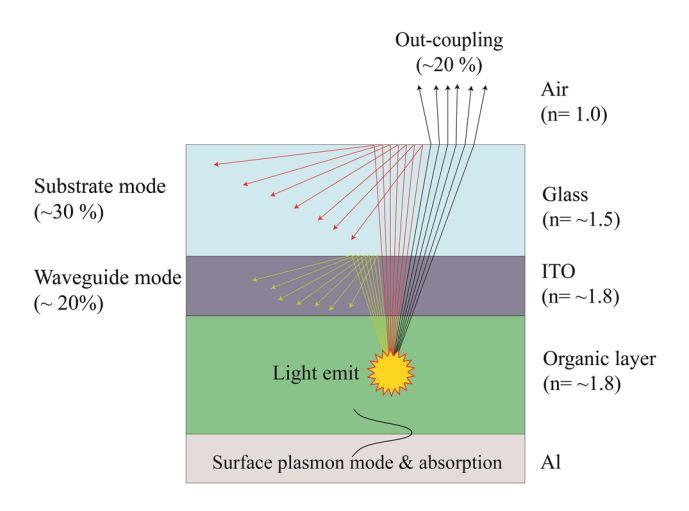


Figure 1: Various optical loss modes such as substrate mode, waveguided mode, and surface plasmon mode in an OLED.

embedding NPs into OLED is a relatively simple method suitable for large-area manufacturing.

In the case of OPV, one of the significant constraints that limit the performance is the effective absorption of incident light and photogeneration of current. However, a large portion of the incident light tends to be reflected at the surface of air and glass, absorbed in electrode, buffer layers, or escape into the air [22]. Therefore, to acquire high-efficiency OPVs, it is important to reduce the optical losses and increase light absorption in the active layer. Optical losses can be reduced by designing a structured back reflector, a structured substrate, and NPs to induce plasmonic effects, scattering, or near-field enhancement [23].

In both the OLED and OPV, a layer between the active layer and the indium tin oxide (ITO) anode layer is added to improve the charge transfer. The layer is known as hole injection layer (HIL) for OLED and the hole extraction layer (HEL) for OPV. Poly(3,4-ethylenedioxythiophene): poly(styrene sulfonate) (PEDOT:PSS) (Figure 2) is the most commonly used HIL or HEL layer for both the devices. PEDOT:PSS is a polyelectrolyte with the combination of electrically conducting conjugated PEDOT (positively charged) and insulating PSS (negatively charged) steadily dispersed in water [24]. Oxidised PEDOT is highly conductive, but it is insoluble in water. The insulated PSS is a polymer surfactant that facilitates PEDOT to disperse in water [25]. PEDOT:PSS is commercialised under the trade name Clevios<sup>TM</sup> formerly known as Baytron P [25]. The PEDOT:PSS aqueous solutions (Clevios) are widely used for preparing highly conductive and flexible electrodes such as Clevios PH500 [25,26] and Clevios PH1000 [27-30]; whereas the less conductive PEDOT:PSS

Figure 2: The chemical structure of PEDOT:PSS.

(Clevios P VP Al 4083 [31–33]) is used as hole injection/ extraction layers. The antistatic coating, solid electrolyte capacitor, and printed circuit board were the first practical applications of PEDOT:PSS [34]. The importance of PED-OT:PSS as a hole injection layer has been documented by many groups [35,36]. Until now, PEDOT:PSS has been extensively reported as being used as a buffer layer in organic optoelectronics [25]. The commercially available PEDOT:PSS is a widely used material for organic optoelectronic owing to its high transparency in the visible range, easy to process, excellent surface morphology, great mechanical flexibility, adjustable conductivity, high work function, and excellent thermal stability [20,37,38]. Nevertheless, higher hole injection and conductivity are beneficial. However, pure PEDOT:PSS having low conductivity, is sensitive to air, and adhere weakly to hydrophobic substrates [37]. One strategy is to incorporate NPs such as gold (Au) NPs [39], silver (Ag) NPs [40], or carbon nanotube [41] into the PEDOT:PSS layer for applications in flexible or even stretchable devices [24]. A few effects improve device efficiencies when NPs are doped into PEDOT:PSS, such as better hole injection, higher conductivity, plasmonic effect, scattering, etc. [39–41].

There are varieties of NPs or nanomaterials available, such as metal-based [13], metal oxides [42], organic-based [27], carbon-based [43], 2D materials [44,45], and hybrid-based NPs [46]. They exhibit unique physical and chemical properties and are used in wide range of fields such as water treatment [47], agriculture [48], biological [49–51], optoelectronics [52], sensors [53], construction materials (cement) [54,55], photocatalyst [56,57], *etc.* Furthermore, NPs can be synthesised into different shapes,

sizes, and structures. It can be spherical, triangle, square, or irregular form. The combination of NPs such as metalmetal, metal-metal oxide, carbon-metal, and organic-metal forms hybrid NPs, which possess synergetic properties of each type of NP [58,59]. Metallic NPs are widely used in organic optoelectronics due to the surface plasmon resonance effect (SPR) or localised surface plasmon resonance (LSPR). At the same time, they also enhanced the transport layer conductivity to improve the overall device performance [4,60,61]. SPR is defined as the resonant oscillation of conduction electrons that occurs between materials with negative and positive permittivity. At the same time, LSPR is light-induced and matches the frequency of the metallic surface, causing free surface electrons to oscillate collectively.

There are few strategies of using NPs on organic optoelectronic devices in terms of the position, which included: (i) between anode and hole injection or extraction layer (ITO/HIL or HEL) [62-64] (Figure 3(a)), (ii) in HIL or HEL [21,40,65,66] (Figure 3(b)), (iii) between active layer and HIL or HEL [67] (Figure 3(c)), and (iv) in active layer [68–70] (Figure 3(d)). In this review, we will be focusing on the NPs embedded into the HIL for OLEDs or HEL for OPVs (Figure 3(b)). The use of NPs at this position has been proposed for light trapping, absorption, re-scattering of light, and a near-field enhancement [71]. The easiest way is to dope the NPs into a hole injection material such as PEDOT:PSS or deposit them at the top of the anode layer.

This review article presents a brief technical summary of the types of NPs embedded into PEDOT:PSS nanocomposite for OLEDs and OPVs. The performances are listed and reviewed. The effects of the NPs in PEDOT:PSS for organic are discussed and summarised. Finally, outlooks and conclusions on nanoparticles-doped PEDOT:PSS for OLEDs and OPVs are drawn.

# 2 NPs-doped PEDOT:PSS for OLED

Incorporation of NPs into PEDOT:PSS has evolved into one of the most common ways to improve OLED performance irrespective of the spectral range. It has been used for blue, red, and green-emitting OLEDs. The typical device configuration has been reported are mostly in ITO(anode)/ NPs:PEDOT:PSS(HIL)/HTL/EML/ETL/EIL/aluminium (Al) (cathode), (Figure 4).

#### 2.1 Metallic-based NPs

The most commonly used metallic NPs are Ag and gold Au with the size of 5-80 nm; the size and concentration are optimised to achieve the best improvement in current efficiency (CE), as shown in Table 1.

In 2012, Mucur et al. synthesised Ag NPs with particles size of around 6 nm diameter and mixed them into

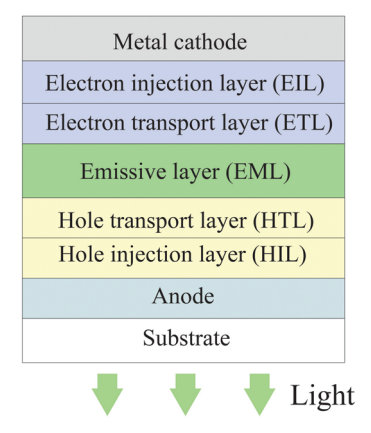


Figure 4: Device structure of a typical OLED with NPs-doped PEDOT:PSS.

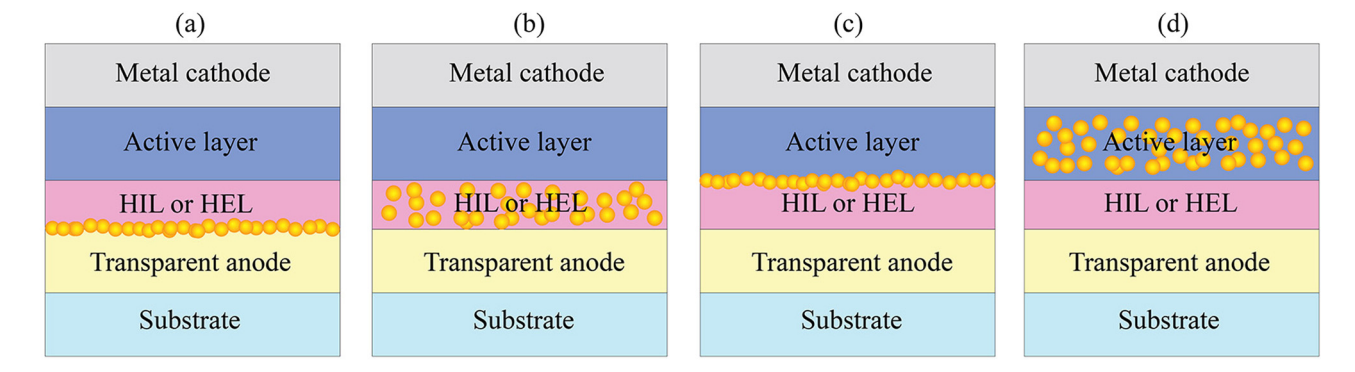


Figure 3: Schematic diagram of device structure with NP in OLEDs and OPVs, (a) between anode and hole injection or extraction layer (ITO/ HIL or HEL), (b) in HIL or HEL (main focus in this review), (c) between active layer and HIL or HEL, and (d) in active layer.

Table 1: Device characteristics of OLEDs with metallic-based NPs-doped PEDOT:PSS

NPs	Size of NP (nm)	Thickness (nm) <sup>(a)</sup>	Function	CE (cd/A)	PE (lm/W)	<b>EQE</b> (%)	Enhance in CE (%) <sup>(b)</sup>	Remarks	Ref.
Ag	6	70	HIL	0.64	_	_	28.90	Improved hole injection	[13]
Ag	30	30	HIL	_	_	0.94	13.25 (EQE)	Improved hole injection	[72]
Ag	60	55	HIL	1.46	_	_	18.70	Improved hole injection and LSPR	[12]
Ag	55	40	HIL	31.00	6.80	8.20	72.20	LSPR	[73]
Cu	21	40	HIL	26.60	6.20	6.30	47.80	LSPR	[73]
Au	20	40	HIL	27.00	7.20	8.00	50.00	LSPR	[73]
Cu and Ag	21 and 55	40	HIL	32.10	7.50	8.30	78.30	LSPR	[73]
Au and Ag	20 and 55	40	HIL	35.30	8.20	9.80	96.10	LSPR	[73]
Au	5	75-80	HIL	15.10	_	_	14.40	SPR	[21]
Au	10	75-80	HIL	16.40	_	_	24.20	SPR	[21]
Au	20	75-80	HIL	17.10	_	_	29.50	SPR	[21]
Au Nanorod	_	75-80	HIL	17.50	_	_	32.60	SPR	[21]
Bio-Au	10.4	50	HIL	1.58	_	1.09	85.90	SPR and scattering	[74]

CE: current efficiency, PE: power efficiency, EQE: external quantum efficiency, HIL: hole injection layer, (-): no data provided. (a): thickness of PEDOT:PSS:NPs composite layer, (b): compared with pristine PEDOT:PSS.

PEDOT:PSS. 12.5 wt% Ag NPs exhibited the highest performance and the increase in CEs by 28.90% is mainly due to more efficient charge injection without affecting the emission colour [13]. In another work, the CE was also improved (~13%) using larger Ag NPs (30 nm) with the concentration of 0.025 wt% Ag NPs doped into PEDOT:PSS, it is attributed to the enhanced hole injection [72]. However, larger size ~60 nm Ag NPs into PEDOT:PSS as HTL was found to exhibit a negligible effect on the hole injection efficiency due to the excitation of LSPR around Ag NPs [12].

The investigation by the same group using copper (Cu), Ag, and Au NPs and also dual metal NPs imbedded into PEDOT:PSS with the device architecture of ITO/NPs-PEDOT:PSS/CBP:Ir(MMPIPA)2(acac)/LiF/Al further confirm the LSPR effects [73]. The optimum particle size and concentration used were Ag (55 nm, 40%), Au (20 nm, 24%), Cu (21 nm, 50%), Cu-Ag (21-55 nm, 62%), and Au-Ag (20-55 nm, 80%), respectively. After doped metal NPs into PEDOT:PSS, all the devices are exhibited better stability due to the alleviated acidic and the hygroscopic nature of PEDOT:PSS. The results also showed that codoped Au and Ag or Cu and Ag for green OLEDs exhibited higher efficiency due to the synergistic effect of stronger near-field resonance of Au NPs and broadband resonance of Ag NPs. In another work, Au NPs of different sizes and shapes were used in PEDOT:PSS composite. At the same time, Au nanorods showed the highest efficiencies compared to the other spherical-shaped Au NPs with the size of 5, 10, and 20 nm. The results suggest that Au NPs with larger size and higher surface area have more obvious "far-field" surface plasmon resonance (FSPR) effects that acquire higher reflectivity [21].

Biologically synthesised gold nanoparticles (Bio-Au NPs) have been introduced into polymer OLEDs. They used microorganisms to grow at high metal ion concentrations. It can eliminate the toxic effect of metals by adjusting the redox state and metal NPs were formed intracellularly from the metal ions. They optimised the bio-Au NPs' concentration with 0.125 wt%, which is improved by 85.90% of the current efficiency compared to the non-doped PEDOT:PSS layer [74].

## 2.2 Inorganic NPs

The investigation of inorganic NPs in PEDOT:PSS for OLED is listed in Table 2. The enhancement of efficiency is mainly attributed to better hole injection. Molybdenum trioxide (MoO<sub>3</sub>) NPs with the optimal volume ratio of PEDOT:PSS to MoO<sub>3</sub> of 3:1 were studied for OLEDs [20]. The composite solution coated as HIL results in a smooth and pin-hole-free morphology compared to the solutionprocessed pure MoO<sub>3</sub>. Another advantage of adding MoO<sub>3</sub> to PEDOT:PSS as HIL possesses a high work function (5.54 eV) compared to the PEDOT:PSS pristing film. The work function is increased by 0.3 eV, which reduced the energy barrier and improved hole injection. In another work, molybdenum disulphide (MoS<sub>2</sub>) was added into PEDOT:PSS as HIL and effectively promoted hole

Table 2: Device characteristics of OLEDs with inorganic NPs-doped PEDOT:PSS

NPs	Size of NP (nm)	Thickness (nm) <sup>(a)</sup>	Function	CE (cd/A)	PE (lm/W)	<b>EQE</b> (%)	Enhance in CE (%) <sup>(b)</sup>	Remarks	Ref.
MoO <sub>3</sub>	3:1 <sup>(c)</sup>	30	HIL	-	89.2	23.9	~84.00 (EQE)	Reduced energy barrier and improved hole injection	[20]
$MoS_2$	2:1 <sup>(c)</sup>	_	HIL	8.10	5.70	4.14	68.75	Promotes conductivity and device durability	[75]
$WO_x$	20:1 <sup>(c)</sup>	_	HIL	_	_	2.30	42.86 (EQE)	Promotes conductivity and device durability	[76]
TiO <sub>2</sub>	25	_	HIL	7.30	3.15	_	760.50	Improved light out-coupling	[79]
ZnO	200 (length)	-	HIL	11.03	4.34	-	138.70	Improved charge mobility and conductivity	[80]

CE: current efficiency, PE: power efficiency, EQE: external quantum efficiency, HIL: hole injection layer, (—): no data provided.

(a): thickness of PEDOT:PSS:NPs composite layer, (b): compared with pristine PEDOT:PSS, (c): ratio of PEDOT:PSS with NPs (PEDOT:PSS:NPs).

injection. MoS<sub>2</sub> incorporation in the PEDOT:PSS matrix contributed to promoting conductivity and improved the device durability for the UV OLEDs. At the same time, the current efficiency of the OLED was improved by 68.75% [75].

In addition, tungsten oxide ( $WO_x$ ) doped into PEDOT: PSS also showed a similar effect that improved hole injection and device durability for the UV OLED devices [76]. The improvement is due to the non-stoichiometry in  $WO_x$  and  $WO_x$ :PEDOT:PSS accompanied by slight oxygen deficiency [77,78], which provides a hole transport channel to promote hole injection or transport in organic electronic devices [76].

Furthermore, commonly used inorganic NPs, titanium dioxide (TiO<sub>2</sub>) NPs (20 wt%, 25 nm), was doped into PEDOT:PSS as HIL, and an impressive improvement in the CE of around 760.5% was found and it was due to the improvement in light out-coupling from light scattering layer [79]. Meanwhile, the same group tested the incorporation of zinc oxide (ZnO) nanorod in PED-OT:PSS [80], a lower improvement (138.7%) was achieved compared to TiO<sub>2</sub>. The ZnO nanocomposite results in strong interaction between ZnO and thiophene rings of

PEDOT:PSS and polymer chains changes from coiled to linear [81].  $\pi$ -electrons are more delocalised in linear PEDOT:PSS; hence, charge mobility and conductivity increase. In addition, it is also possible for nanostructured ZnO to enhance light out-coupling [80].

#### 2.3 Carbon-based NPs

Recently, carbon-based NPs or nanomaterials have been widely used as transparent conducting films (TCFs) [82] in optoelectronic devices [29,37]. Carbon nanomaterials such as nanotubes, graphene, and graphene oxide (GO) have been investigated as substitutes for ITO (Table 3). For example, graphene possesses high transmittance and conductivity, and exhibits optical transmittance comparable to ITO at visible wavelengths [82]. A highly efficient ITO-free OLEDs were obtained by using PEDOT:PSS:GO as an anode with the device configuration of anode/NPB/Alq3/LiF/Al [83]. The highest CE of the device (PED-OT:PSS:GO with the ratio of 15:1) is 5.71 cd/A, while for pristine PEDOT:PSS layer is only 3.47 cd/A; thus, a 55%

Table 3: Device characteristics of OLEDs with carbon-based NPs-doped PEDOT:PSS

NPs	Concentration	Thickness (nm) <sup>(a)</sup>	Function	CE (cd/A)	PE (lm/W)	<b>EQE</b> (%)	Enhance in CE (%) <sup>(b)</sup>	Remarks	Ref.
GO	15:1 PEDOT:PSS/GO	57	Anode	5.71	_	-	55.00	Improved hole injection	[83]
PRPOHA-GO	(2 mg/mL; in EG) 15:1 v/v	44	Anode	~0.11	~0.06	~0.10	~1.60 <sup>(c)</sup>	Lower resistivity	[28]

CE: current efficiency, PE: power efficiency, EQE: external quantum efficiency, (-): no data provided.

<sup>(</sup>a) thickness of PEDOT:PSS:NPs composite layer, (b) compared with pristine PEDOT:PSS, and (c) compared to ITO.

enhancement was obtained. This improvement indicates that PEDOT:PSS:GO composite possibly reduces the energy level difference, hence better hole injection [84]. Graphene oxide sheets are vigorously oxidised by hydroxyl and epoxide groups, and it helps assemble other materials through  $\pi$ - $\pi$  stacking and hydrogen bonding [85]. Therefore, GO-doped PEDOT:PSS is able to promote the interaction between GO and PEDOT but not PSS due to the electronegativity of GO.

On the other hand, several amines such as n-propylamine (nPRYLA), dipropylamine (DPRYLA), and propanolamine (PRPOHA) have been used to modify GO and doped into PEDOT:PSS (PH1000) with additional ethylene glycol (15:1) used as anode [28]. The device structure is anode/PEDOT:PSS(Al4083)/ADS231BE/Cs<sub>2</sub>CO<sub>3</sub>/Al. All the devices show enhancement in CE, PE, and EQE (1.6-, 1.5-, and 1.9-fold enhancement, respectively) compared to the device with ITO anode. PRPOHA-GO was the best device among the amine-modified GO devices due to lower surface resistivity.

# 2.4 Hybrid NPs

Hybrid NPs are defined as when two or more distinct NPs are assembled but still in nanoscale dimensions. Hybrid NP systems can be obtained by combining two different materials such as organic-inorganic, decorated-metal oxide NPs, metal-metal oxide, and core-shell to obtain unique or synergetic properties [58,59].

When PdCo alloy NPs supported on polypropylenimine dendrimer-grafted graphene (PdCo/PPI-g-G) with 0.02 wt% was doped into PEDOT:PSS, the highest luminous efficiency (2.36 cd/A) and luminous PE (0.11 lm/W) were obtained for poly(9,9-di-n-octylfluorenyl-2,7-diyl) (PFO)based blue OLED. When PdCo/PPI-g-G is doped in PEDOT:PSS, the energy barrier between the ITO anode and the PEDOT:PSS is around 0.5 eV. At low doping concentrations of 0.02 wt% PdCo/PPI-g-G, the luminance improvement was related to an increase in hole injection, which led to a better balance of electron/hole in the PFO layer. However, further increase in the concentration of PdCo/PPI-g-G (>0.02 wt%) shifted the recombination zone toward to cathode; thus, the luminescence efficiency was decreased [86].

Several studies have been carried out using a combination of a metal core with organic material outer shell doped PEDOT:PSS. Polystyrene (PS)-coated gold core-shell NPs (Au@PS NPs) were studied in green phosphorescent OLEDs with the device configuration of glass/

ITO/Au@PS NPs-PEDOT:PSS/PVK:PBD:Ir(PPy)3/LiF/Al. It improved the current efficiency by 42.36% compared to the device with a bare PEDOT:PSS layer. At ambient conditions, the cross-linked PS shell for Au@PS NPs provided hydrophobic and structural stability by ensuring their structural stability against oxidation and minimising the adverse effect of the hygroscopic and acidic PEDOT:PSS film on the organic electronic devices. By using emulsion polymerisation, Au NPs were encapsulated in PS shells. The thickness of PS shell is tunable to optimise plasmonic coupling efficiency between the Au NPs and the emitting or active layers [1]. In another similar work, smaller Ag NPs (3-6 nm) were encapsulated with organic material (o-phenylenediamine [o-PDA]). o-PDA@Ag NPs displayed a surface plasmon absorption band cantered at 448 nm. The improvement is due to the insulating NPs attributed to the film morphology change and enhanced balance of injected electrons and holes. The device consisting of o-PDA@Ag NPs exhibited ~20% improvement in current efficiency compared to pristine PEDOT:PSS as HIL [87].

Magnetic NPs have recently been reported as a holetransport layer for OLEDs. Magnetic NPs induce tuning the ratio of singlet to triplet excitons in the emissive layer [88]. In addition, the combination of magnetic NPs Iron(II,III) oxide – Fe<sub>3</sub>O<sub>4</sub>) with other materials Fe<sub>3</sub>O<sub>4</sub>@G, Fe<sub>3</sub>O<sub>4</sub>@SiO<sub>2</sub>, and Fe<sub>3</sub>O<sub>4</sub>@Au have also been studied [89]. Fe<sub>3</sub>O<sub>4</sub> are modified by graphene (G), silicon dioxide (SiO<sub>2</sub>), and Au nanoclusters, respectively, then mixed with the PEDOT:PSS as HIL. The nanocomposite serves as a lightout coupling layer that contributes to EQE enhancement by combining magnetic, localised surface plasmon resonance, and scattering effects. Compared to bare PEDOT:PSS, the current efficiency enhancement for Fe<sub>3</sub>O<sub>4</sub>@G, Fe<sub>3</sub>O<sub>4</sub>@SiO<sub>2</sub>, and Fe<sub>3</sub>O<sub>4</sub>@Au are 8.2, 27.1, and 35%, respectively. This enhancement has also been observed in carbon-coated magnetic alloy NPs (CoPt and FePt) [90]. Introducing GO-silver nanowire (AgNWs) [69] and also Ti<sub>3</sub>C<sub>2</sub>T<sub>x</sub> (MXene)-nanosheet-AgNW [91] doped into PEDOT:PPS as anode can lower the sheet resistance, smoothen the surface roughness as compared to AgNWs:PEDOT:PSS or pristine AgNWs layer [69,91]. The enhanced luminescence intensity is also attributed to the SPR effect from the AGNW, thereby reducing the waveguide loss by light scattering [69]. A summary of the data is presented in Table 4.

# 3 NPs-doped PEDOT:PSS for OPVs

Many groups have reported incorporating NPs into OPV to improve the performance of OPVs by inducing plasmonic

Table 4: Device characteristics of OLEDs with hybrid NPs-doped PEDOT:PSS

NPs	Size of NP (nm)	Thickness (nm) <sup>(a)</sup>	Function	CE (cd/A)	PE (lm/W)	EQE (%)	Enhance in CE (%) <sup>(b)</sup>	Remarks	Ref.
PdCo/PPI-g-G Au@PS	0.02 wt% <sup>(e)</sup> 34 (core) 100 (outer)	5 —	HIL HIL	2.36 28.90	0.11 6.50	- 7.80	223.29 42.36	High hole injection SPR	[86] [1]
o-PDA@Ag Fe <sub>3</sub> O <sub>4</sub> @G	3–6 8.6	40 —	HIL HIL	~2.10 4.11	- 3.16	- 1.35	~20.00 8.20	Improved hole injection Magnetic, LSPR, and scattering	
Fe₃O₄@SiO₂ Fe₃O₄@Au C-FePt	15.8 19.7 11.5	_ _ 40	HIL HIL HIL	4.83 5.13 5.40	4.27 3.5 2.20	1.59 1.73 1.83	27.10 35.00 47.10	Magnetic, LSPR, and scattering Magnetic, LSPR, and scattering Magnetic, LSPR, and scattering	[89] [89] [90]
C-CoPt GO-AgNW	3.4 AgNW 5 µm (length) and 50 nm (dia.)	40 —	HIL Anode	5.45 6.20	3.15	1.84	21.30 47.62 <sup>(c)</sup>	Magnetic, LSPR, and scattering Lower sheet resistance, smoothened surface	[90] [69]
AgNW-MXene	AgNW 22 nm (dia.)	_	Anode	21.0	_	25.9	766.70 <sup>(d)</sup>	roughness, and scattering Lower sheet resistance, smoothened surface roughness, and scattering	[91]

CE: current efficiency, PE: power efficiency, EQE: external quantum efficiency, HIL: hole injection layer, (—): no data provided, dia.: diameter. (a): thickness of PEDOT:PSS:NPs composite layer, (b): compared with pristine PEDOT:PSS, (c): compared with ITO, (d): compared with bare AgNW, and (e): concentration.

effects, increasing light absorption, enhancing the rate of exciton generation, or increasing multiple scattering events, thereby enhancing light absorption efficiency [39,92]. Most of the reported device configuration for OPVs is based on ITO(anode)/PEDOT:PSS(HIL)/BHJ(active layer)/EIL/Al(cathode). P3HT:PCBM blends are commonly used as the active layer for OPV, (Figure 5).

#### 3.1 Metal NPs

Metal NPs, especially Ag NPs and Au NPs, are most commonly embedded into PEDOT:PSS to enhance efficiency [4,60,61] (Table 5). Ag NPs usually have an absorption

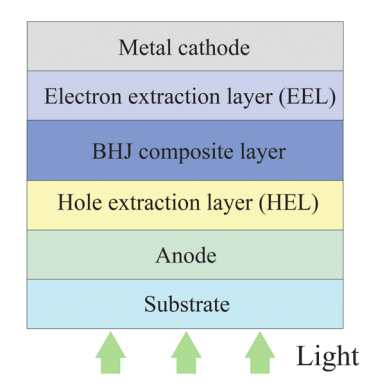


Figure 5: Device structure of a typical OPV with NPs doped into PEDOT:PSS.

peak between 400 and 450 nm, and Au NPs have an SPR peak between 500 and 600 nm, which relies on the thickness, shape, and distance of the nano-structures [93]. When decahedral and icosahedron of Ag NPs are doped into PEDOT:PSS as hole extraction layer [94], the absorption peaks for decahedral Ag NPs (50-65 nm) are at 407 and 502 nm, while the absorption peak of icosahedron Ag NPs (30-40 nm) is at 412 nm, indicating that the decahedral Ag NPs have a wider light-harvesting range than icosahedron Ag NPs. The AFM measurements revealed that the PEDOT:PSS:Ag-decahedral NPs composite film had a higher roughness, improving the cell's hole collection efficiency because larger particles lead to a stronger plasmonic scattering effect. It results in an improvement of 12.10% as compared to PEDOT:PSS layer. Meanwhile, improvements in the efficiency of CuPc/C60 solar cells with various AgNP sizes (43, 45, 51, 54, and 57 nm) have been observed [40]. Among the particle sizes tested, 57 nm had the highest power conversion efficiency (PCE) at ~0.93%, owing to the SPR effect, which can decompose the excitons electron-hole pair into e<sup>-</sup> and h<sup>+</sup> that have moved to the cathode and anode of the cell, which is affecting the efficiency.

In another report, 80 nm Ag NPs with a spherical shape dispersed in PEDOT:PSS were then fabricated into P3HT:PCBM-based organic solar cells [32]. The Ag NPs are nearly spherical and distributed uniformly on the glass surface; no apparent aggregation is observed. Compared to pure PEDOT:PSS, PEDOT:PSS incorporated with Ag NPs

Table 5: Device characteristics of OPVs with metallic-based-NPs doped PEDOT:PSS

NPs	Active layer	Size of NP (nm)	Thickness (nm) <sup>(a)</sup>	Function	FF (%)	PCE (%)	Enhance in PCE (%) <sup>(b)</sup>	Remarks	Ref.
Ag	PTB7:PC <sub>71</sub> BM	50-65	40	HEL	63.20	6.50	12.10	Better hole collection	[94]
Ag	CuPc:C60	57	_	HEL	39.70	0.93	_	SPR	[40]
Ag	P3HT:PCBM	80	55	HEL	38.80	2.65	16.20	Higher conductivity	[32]
Ag	P3HT:PCBM	20-40	40	HEL	51.20	3.20	8.50	SPR and improved hole collection	[26]
Au	P3HT:PCBM	_	40	HEL	51.50	3.19	8.50	SPR and improved hole collection	[26]
Ag	rrP3HT: PC <sub>61</sub> BM	10	40	HEL	62.00	4.94	5.55	SPR, increases absorption length and scattering	[95]
Au	rrP3HT: PC <sub>61</sub> BM	20	40	HEL	62.00	4.99	6.62	SPR, increases absorption length and scattering	[95]
Ag	rrP3HT: PC <sub>71</sub> BM	10	40	HEL	61.00	5.29	6.65	SPR, increases absorption length, scattering	[95]
Au	rrP3HT: PC <sub>71</sub> BM	20	40	HEL	61.00	5.65	13.91	SPR, increases absorption length and scattering	[95]
Au	P3HT:PCBM	11 ± 3	30	HEL	53.30	3.23	32.40	enhanced extraction of charge in hole transport layer	[99]
Au	CuPc/C60	12-23	_	HEL	49.00	1.02	30.80	SPR and improved hole collection	[96]
Au	P3HT:PC <sub>70</sub> BM	18	40	HEL	69.21	3.51	18.50	SPR and improved hole collection	[97]
Au	P3HT:PCBM	45 ± 5	50	HEL	70.32	4.24	18.80	SPR and improved hole collection	[4]
Au	P3HT:PCBM	14 ± 4	_	HEL	30.02	1.00	66.67	SPR and improved hole collection	[98]
Au	P3HT:PC <sub>60</sub> BM	50	30	HEL	66.10	4.14	15.00	Stronger near-field enhancement, thus higher photocurrent output	[101]
Au	PBDT-TS1:PC <sub>70</sub> BM	50	30	HEL	67.34	10.29	27.98	Stronger near-field enhancement, thus higher photocurrent output	[101]
Au and Ag	PTB7:PC <sub>70</sub> BM	40 and 50	60	HEL	69.00	8.67	19.60	Absorption enhancement and broadens the wavelength range	[102]
Au and Ag	rrP3HT:PC <sub>61</sub> BM	10 and 20	40	HEL	62.00	5.31	_	SPR and absorption enhancement	[103]
Au and Ag	rrP3HT:PC <sub>71</sub> BM	10 and 20	40	HEL	50.00	5.71	_	SPR and absorption enhancement	[103]

FF: field factor, PCE: power conversion efficiency, HEL: hole extraction layer, (-): no data provided. (a): thickness of PEDOT:PSS:NPs composite layer, (b): compared with pristine PEDOT:PSS.

exhibit an increase in PCE up to 16.20%. The author clarified that LSPR is not the origin of efficiency; the concentration of Ag NPs (80 nm) (0, 0.1, and 1 wt%) with PEDOT:PSS composite films show almost similar transmittance ~90% at the wavelength 300-800 nm, which means the concentration of Ag NPs has no apparent impact on the optical effects. The PEDOT:PSS layer incorporated with Ag NPs exhibited higher conductivity that contributed to PSC improvement. Besides, another study reported the effect of Ag Nps- or Au Nps doped PEDOT:PSS composite as hole extraction layer compared with pristine

PEDOT:PSS with the device configuration of ITO/Composite layer/P3HT:PCBM/LiF/Al [26]. PCE was improved by 8.5% for both Ag NPs and Au NPs in the  $20-40\,\mathrm{nm}$  size range, which was attributed primarily to the SPR effect and improved hole extraction by increasing surface roughness at the buffer layer [26].

Furthermore, a detailed comparison of PEDOT:PSS + Au NPs and PEDOT:PSS + Ag NPs with the average particle size for Ag NPs (~10 nm) and Au NPs (~20 nm) was reported [95]. The absorption peaks of Au NPs and Ag NPs were observed at 521 and 431 nm. The optimised

OPV device structure for both metal NPs is fabricated with a configuration of ITO/PEDOT:PSS + metal NPs/ rrP3HT:PC<sub>61</sub>BM/BCP/LiF/Al and ITO/PEDOT:PSS + Metal NPs/rrP3HT:PC<sub>71</sub>BM/BCP/LiF/Al. The surface roughness of the bare pristine PEDOT:PSS layer was around 2.61 nm, whereas the PEDOT:PSS + Au NPs composite and the PED-OT:PSS + Ag NPs composite was 2.69 and 3.56 nm, respectively. Ag NPs and Au NPs have better performance for both BHJ structures than the bare PEDOT:PSS. The PCE improvement in PEDOT:PSS + Ag NPs and Au NPs with rrP3HT:PC<sub>61</sub>BM were 5.55 and 6.62%, respectively, whereas 6.65 and 13.91% for PEDOT:PSS + Ag NPs and Au NPs with rrP3HT:PC<sub>71</sub>BM. The surface plasmon effect for metal NPs increases photo absorption length, scattering, and trapping of incident light passing through the HIL. Compared to the device's performance for both PEDOT:PSS + Ag NPs and PEDOT:PSS + Au NPs, the devices with PEDOT:PSS + Au NPs showed better results due to the absorption range of Au NPs, which absorbed more in visible range [95].

In recent years, incorporating Au NPs with PEDOT: PSS in different OPV device configurations and different Au NPs sizes have resulted in performance enhancement with optimised Au-NPs concentration in PEDOT:PSS [4,95–99]. They shared a similar outcome where Au NPs enhanced charge extraction in the hole transport layer; thus, the energy barrier was lowered and promoted carrier transport [99,100]. Besides that, Au NPs have unique optical properties of the LSPR that enhance the light absorption efficiency to improve the performance of the OPVs [4,96,97]. Optimising the concentration of Au NPs in PEDOT:PSS is important as above a concentration threshold, the additional leakage current was detected resulting from increased defects in the hole transport layer that act as a recombination centre [99]. A fairly high increment of PCE efficiency can be achieved

when Au NPs are doped into PEDOT:PSS as hole extraction layer and compared to control devices (bare PEDOT:PSS); 32.4% [99], 30.8% [96], 18.5% [97], 18.8% [4], 66.67% [98], 15.00% [101], and 27.98% [101], respectively. Furthermore, by taking advantage of both Ag NPs and Au NPs with different absorption regions, a mixture of AgNps and Au NPs showed even better solar cell performance than only a single type of metal NPs. EQE spectra and UV-vis absorption spectra for dual NPs showed absorption enhancement compared with single NPs and without NPs with a broader absorption spectrum [102]. The highest PCE value is 5.71% with  $J_{sc} = 16.44 \text{ mA/cm}^2$  for an optimised ratio of Au NPs (10 nm):Ag NPs (20 nm) (25:75) in PEDOT:PSS which consisted of devices architecture of ITO/PEDOT:PSS + Au NPs:Ag NPs(25:75)/rr-P3HT:PC<sub>71</sub>BM/BCP:LiF:Al, whereas, for ITO/PEDOT:PSS + Au NPs:Ag NPs(25:75)/rr-P3HT:PC<sub>61</sub>BM/ BCP:LiF:Al the best PCE was 5.31% with  $J_{sc} = 14.77 \text{ mA/cm}^2$ [103].

#### 3.2 Organic NPs

Another strategy to further improve the performance of OPV is using organic NPs as listed in Table 6. Crosslinked PS NPs are able to enhance the mechanical durability of flexible electronics [27]. A flexible organic solar cell was investigated using the stamping process of the PEDOT:PSS layer with PSNPs. The PSNPs with a particle size of 68 nm are doped into PEDOT:PSS and diluted by IPA, then spin-coated onto the polyurethane acrylate (PUA)/PC stamp and stamped onto the PH1000/PEN substrate. The complete device structure is PEN/PEDOT:PSS/ PEDOT:PSS:PS NPs/PTB7:PC<sub>71</sub>BM/TiO<sub>x</sub>/Al; the processes are illustrated in Figure 6. The stamped PEDOT:PSS:PS

Table 6: Device characteristics of OPVs with organic NPs-doped PEDOT:PSS

NPs	Active layer	Size of NP (nm)	Thickness (nm) <sup>(a)</sup>	Function	FF (%)	PCE (%)	Enhance in PCE (%) <sup>(b)</sup>	Remarks	Ref.
PS	PTB7:PC <sub>71</sub> BM	68	30	HEL	0.52	5.71	0.70	Lowered work function and better device mechanical stability	[27]
PPy	PTB7:PC <sub>61</sub> BM	30	40	HEL	67.93	3.35	15.12	Changes in pH value, increase in conductivity, and morphological changes	[104]
PPy	PTB7:PC <sub>71</sub> BM	30	40	HEL	71.06	9.44	17.90	Changes in pH value, increase in conductivity, and morphological changes	[104]

FF: Field factor, PCE: power conversion efficiency, HEL: hole extraction layer, (-): no data provided.

<sup>(</sup>a): thickness of PEDOT:PSS:NPs composite layer, (b): compared with pristine PEDOT:PSS.

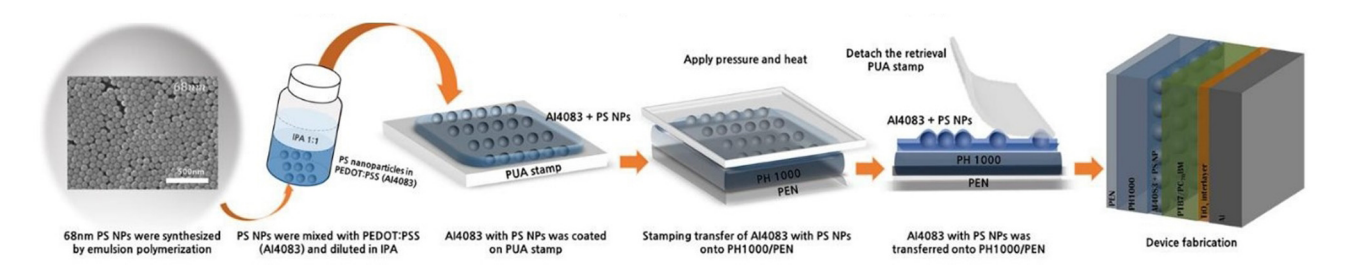


Figure 6: The stamping transfer process of the PPy NPs:PEDOT:PSS layer for PTB7/PC<sub>71</sub>BM based flexible solar cell [27]; Copyright (2018) Royal Society of Chemistry.

NPs exhibited significant mechanical stability enhancement when undergoing a bending test. At the same time, the work function of the PEDOT:PSS:PS NPs provided by stamping is 5.09 eV which is lower than the usual spin-coated process for PEDOT:PSS at 5.20 eV. The PED-OT:PSS:PSNP samples possess the highest occupied molecular orbital (HOMO) energy level of 5.15 eV; thus, it has a slightly better hole transport than that of spin-coated PEDOT:PSS. The transferred PEDOT:PSS:PS NPs have the best PCE at 5.71% for PTB7:PC71BM based flexible solar cells and the spin-coated device is only 5.37%. Furthermore, the transferred PEDOT:PSS:PS NPs layer of the flexible organic solar cell device with 1,000 cycles of bending test and retained 65% of its initial efficiency, outperforming the spin-coated PEDOT:PSS device without PS NPs, which retained only 42% of its initial efficiency [27].

Besides that, an impressive PCE of 9.48% was obtained for PTB7:PC71BM based solar cells when watersoluble polypyrrole NPs (PPy NPs) doped PEDOT:PSS was used as buffer layer [104]. PTB7:PC71BM based solar cell was coated a 20% PPy NPs doped PEDOT:PSS layer and obtained a PCE of 9.44%. Comparing this to the pristine PEDOT:PSS and without PEDOT:PSS layer, an improvement of 18 and 152% was achieved. Besides, PTB7:PC<sub>61</sub>BM based solar cells also improved by 15 and 154% compared to the pristine PEDOT:PSS and without the PEDOT:PSS layer, respectively. Notably, the conductivity of 20% PPy NPs:PEDOT:PSS film with  $2.22 \times 10^{-4} \pm 0.2 \times 10^{-4}$  S/cm is 4 times higher than pristine PEDOT:PSS. The pH value of 2.2 for pure PED-OT:PSS is modified to pH value of 7.4, when 20% PPy NPs doped into PEDOT:PSS. The composite is neutralised, while the conductivity and its long-term stability are improved, where hole extraction is much better, and the damage to the ITO surface is lower than the device with pure PED-OT:PSS. Aside from that, the PPy NPs:PEDOT:PSS composite film exhibits phase separation and a bicontinuous interpenetrating network, which are useful for hole transport [104].

## 3.3 Inorganic NPs

Inorganic semiconductors have shown excellent electronic properties, for example, high dielectric constant, high charge mobility, and thermal stability, while the NPs also exhibit enhanced electronic, photo-conducting, and luminescent properties [105]. The reported work for devices using inorganic NPs doped into PEDOT:PSS is presented in Table 7. An increase in efficiency is observed in small molecule OPVs by incorporating TiO2 NPs with PEDOT:PSS as transparent electrode [106]. With 0.5 wt% TiO<sub>2</sub> mixed with PEDOT:PSS, higher transmittance is obtained as compared to the bare PEDOT:PSS layer. The device with the optimised concentration of TiO<sub>2</sub> in PED-OT:PSS showed the best PCE of 7.92%, improved by a factor of 1.08 compared to bare PEDOT:PSS devices. TiO2 NPs act as a scattering volume for increased light coupling for OPV devices and the composite layer also enhances mechanical flexibility. Next commonly used vanadium pentoxide (V2O5) NPs have been studied for the effect of carrier mobility, hole-only devices with different HTLs [107]. In this study, for the embedded V<sub>2</sub>O<sub>5</sub>NPs in PEDOT:PSS layer, the hole mobility  $(\mu_h)$  was calculated according to the Mott-Gurney law. The value of  $\mu_{
m h}$ increases from  $2.54 \times 10^{-4} \, \text{cm}^2 \, \text{v}^{-1} \, \text{s}^{-1}$  for  $V_2 O_5$  and  $3.19 \times 10^{-4} \text{ cm}^2 \text{ v}^{-1} \text{ s}^{-1}$  for PEDOT:PSS to  $4.19 \times 10^{-4} \text{ cm}^2 \text{ v}^{-1} \text{ s}^{-1}$ for V<sub>2</sub>O<sub>5</sub> NPs:PEDOT:PSS. The larger hole mobility can promote charge transfer to enhance photocurrent  $I_{SC}$ and fill factor (FF). Notably, wide-angle X-ray scattering (GIWAXS) revealed a stronger lamellar intensity and  $\pi$ - $\pi$ peaks in the active layer for V<sub>2</sub>O<sub>5</sub> NPs:PEDOT:PSS compared to the pristine PEDOT:PSS layer, further proof that the crystallinity of the active layer (PTB7-Th:PC71BM) coated on the V<sub>2</sub>O<sub>5</sub> NPs:PEDOT:PSS is enhanced. Therefore, V<sub>2</sub>O<sub>5</sub> NPs:PEDOT:PSS acquired a PCE of 9.44% (improved by 14.70%).

Another paper used inorganic oleylamine-functionalised molybdenum disulphide (FMoS<sub>2</sub>) nanosheets doped into PEDOT:PSS as hole extraction layer for P3HT:PCBM

Table 7: Device characteristics of OPVs with inorganic NPs doped into PEDOT:PSS

NPs	Active layer	Size of NP (nm)	Thickness (nm) <sup>(a)</sup>	Function	FF (%)	PCE (%)	Enhance in PCE (%) <sup>(b)</sup>	Remarks	Ref.
TiO <sub>2</sub>	DCV5T-Me:C60	100	-	Anode	60.0	7.92	8.60	Scattering and better mechanical flexibility	[106]
$V_{2}O_{5}$	PTB7-Th:PC <sub>71</sub> BM	0.5% v/v <sup>(c)</sup>	_	HEL	70.14	9.44	14.70	Promotes hole mobility	[107]
$FMoS_2$	P3HT:PCBM	~6.7 nm <sup>(d)</sup>	_	HEL	62.24	3.74	15.10	Lower series resistance	[108]
MoO <sub>3</sub>	P3HT:PC <sub>61</sub> BM	5	30	HEL	63.00	3.29	7.87 <sup>(f)</sup>	Improved wettability and film-forming ability on the polymer surface	[109]
$WO_x$	PBDB-TF:IT-4F	1:1 <sup>(e)</sup>	42	HEL	80.79	14.57	9.63	Increased surface free energy	[110]
WS <sub>2</sub>	PM6:Y6	3% <sup>(g)</sup>	40	HEL	73.50	15.67	9.20	Increased WF and increased hole mobility	[112]

FF: field factor, PCE: power conversion efficiency, HEL: hole extraction layer, (-): no data provided.

(a): thickness of PEDOT:PSS:NPs composite layer, (b): compared with pristine PEDOT:PSS, (c): volume ratio of NPs, (d): FMoS<sub>2</sub> film thickness, (e): ratio of PEDOT:PSS with NPs (PEDOT:PSS:NPs), (f) compared with only e-MoO<sub>3</sub> layer, and (g): volume ratio of WS<sub>2</sub> nanosheet.

based organic solar cell [108]. Introducing a 2D sheet-like FMoS<sub>2</sub> into PEDOT:PSS would increase surface hydrophobicity and facilitate the subsequent deposition of the hydrophobic active layer. The device with FMoS2:PE-DOT:PSS as HTL has lower sheet resistance  $(R_S)$  and higher shunt resistance ( $R_{SH}$ ) than PEDOT:PSS. Therefore, FMoS<sub>2</sub>:PEDOT:PSS films exhibited a PCE of 3.74%, which is 15.1% higher than the reference device with only PEDOT:PSS layer. In another work, the author demonstrated MoO<sub>3</sub> mixed with PEDOT:PSS as hybrid ink resulted in better wettability and forming a smoother surface. The film-forming ability of the MoO3:PEDOT:PSS hybrid ink was improved due to the stronger bonding between the MoO<sub>3</sub> NPs and the photoactive layer. The PCE for MoO<sub>3</sub>: PEDOT:PSS is improved by 7.87% as compared to only  $MoO_3$  layer [109].

Furthermore, WO<sub>x</sub>NPs blended with PEDOT:PSS as HTL can improve device efficiency and surface free energy (yS) [110]. The morphology of BHJ films depends highly on the surface free energy of the underlying interfacial layer [111]. Surface free energies of WO<sub>x</sub>, WO<sub>x</sub>:PEDOT:PSS, and PEDOT:PSS HTLs were calculated to be 73.98, 62.09, and 59.30 mN/m, respectively. The introduction of WO<sub>x</sub>NPs to PEDOT:PSS affected the work function and surface roughness and increased the surface free energy. Based on the optimised WO<sub>x</sub>:PEDOT:PSS composite layer, an impressive PCE of 14.57% with FF near 81% is achieved, mainly due to efficient carrier extraction, leading to reduced nonradiative recombination [110]. In addition, tungsten disulphide nanosheet (WS2NS) was produced using a low-cost liquid-phase exfoliation method [112]. Incorporating WS<sub>2</sub>NS into PEDOT:PSS improved the work function to form an Ohmic contact between the

photoactive layer and the anode. At the same time, WS<sub>2</sub>NS increased the hole mobility and lower charge carrier-recombination in PM6:Y6 based OPV.

#### 3.4 Carbon-based NPs

Carbon-related nanomaterials usually possess high conductivity; thus, the series resistance can be improved when doped into PEDOT:PSS layer. The related works are summarised in Table 8. When multi-walled carbon nanotube (MWCNT) with an optimum concentration of 0.04 wt% was doped into PEDOT:PSS, the PCE improvement of 12.7% was achieved as compared to bare PED-OT:PSS as a result of enhanced conductivity that led to a lower series resistance of the device [43]. However, at higher MWCNTs concentration (>0.2 wt%), the transmittance of the composite film was dropped from 93.2 to 86.2%. The MWCNTs-doped PEDOT:PSS OPV device showed an improvement in overall performance, including short-circuit current density, fill factor, and power conversion efficiency from 8.82 to 9.03 mA/cm<sup>2</sup>, 0.43 to 0.474, and 2.12 to 2.39% as compared to the device with a bare PEDOT:PSS layer. Besides, CNT-related materials, ultra-large GO-PEDOT:PSS was tested as a hole extraction layer with the device configuration ITO/PEDOT:PSS:GO/ P3HT:PCBM/LiF/Al [113]. Optimised power conversion efficiencies of PEDOT:PSS:GO (0.04 wt%) with 6 wt% dimethyl sulfoxide (DMSO) is improved by 13.6%. When DMSO is added to the PEDOT:PSS solution, the PEDOT and PSS chains separate. The coulombic attraction of the PEDOT and PSS chains is weakened; thus, the coulombic repulsions among the positive or negative charges in the

Table 8: Device characteristics of OPVs with carbon-based NPs doped PEDOT:PSS

NPs	Active layer	Concentration	Thickness (nm) <sup>(a)</sup>	Function	FF (%)	PCE (%)	Enhance in PCE (%) <sup>(b)</sup>	Remarks	Ref.
MWCNT	P3HT:PCBM	0.04 wt%	90-100	HEL	47.40	2.39	12.70	Enhanced conductivity	[43]
GO	P3HT:PCBM	0.04 wt%	_	HEL	62.80	3.39	13.60	<b>Enhanced conductivity</b>	[113]
GO	P3HT:PCBM	_	40	HEL	43.00	3.80	81.00	Enhanced hole collection	[114]
SWCNTs + HClO <sub>4</sub>	PTB7:PC <sub>71</sub> BM	(10:1) + (0.1 M)	100	Cathode	54.00	8.60	15.40 <sup>(c)</sup>	Improved interfacial layer contact and conductivity	[29]

FF: field factor, PCE: power conversion efficiency, HEL: hole extraction layer, (—): no data provided. (a): thickness of PEDOT:PSS:NPs composite layer, (b): compared with pristine PEDOT:PSS, (c) compared with ITO.

PEDOT or PSS chain become the dominant factor for the chain conformation and shift to the linear and extended-coil conformations. At the same time, GO functional groups (–COOH and –OH) also effectively separate PSS and PEDOT chains, which helps the PEDOT and PSS chains to form linear and extended-coil conformations. The linear PEDOT chains have stronger inter-chain interactions, which facilitate charge transport between the chains. Therefore, the conductivity of PEDOT:PSS doped with GO increases. In another report with PEDOT:PSS: GO composite, pre-annealing of GO sheets significantly improves the hole collection ability of the PEDOT:PSS buffer layer, and PCE achieved was 3.8% [114]. The value is 1.8 times better than a pristine PEDOT:PSS buffer layer.

Apart from using carbon-based nanomaterials-PEDOT: PSS as a hole extraction layer, the composite layer has also been studied as an anode. A stable flexible inverted organic solar cell with  $\rm HClO_4$  (0.1 M) doped printed PEDOT-SWCNT films on a PET substrate with the device configuration of PET/PEDOT-SWNTs + (0.1 M)  $\rm HClO_4/PTB7:PC_{71}BM/VO_x$ -PEDOT-PSS/Ag structure has been studied [29]. The bottom electrode (PEDOT:PSS-SWNTs + (0.1 M)  $\rm HClO_4$ ) and  $\rm VO_x$ -PEDOT:PSS film interface layers

were printed with digital materials deposition (DMD), while the PTB7:PC71BM active layer is deposited by spin coating and the Ag electrode by thermal evaporation. Using PEDOT-SWCNTs +  $(0.1\,\mathrm{M})$  HClO4 as a cathode, better performance and stability are obtained compared to the device based on ITO as an anode. SWNTs increased conductivity by adding a small percentage of HClO4 to improve further the interfacial contact with the electron transporting layer and enhance adhesion to PET substrate. PEDOT:PSS:SWNTs:HClO4 as transparent electrode and VOx-PEDOT:PSS as hole transport layer showed the best PCE of 8.6%, which is about 15.4% improvement as compared to ITO.

## 3.5 Hybrid NPs

A wide variety of hybrid NPs, such as bimetallic noble metal or metal/metal oxide hybrid nanoparticles, or organic capped metal NPs have been explored for OPV. These special class NPs are gaining interest since the hybrid NPs possess the properties of both the materials (Table 9). The hybridisation of the two distinct NPs can lead

Table 9: Device characteristics of OPVs with hybrid NPs doped PEDOT:PSS

NPs	Active layer	Size of NP (nm)	Thickness (nm) <sup>(a)</sup>	Function	FF (%)	PCE (%)	Enhance in PCE (%) <sup>(b)</sup>	Remarks	Ref.
PEG-capped Au	РЗНТ:РСВМ	18	30	HEL	62.0	3.51	13.20	Higher roughness and better hole collection	[115]
Cu-Au	P3HT:PC <sub>61</sub> BM	50	40	HEL	52.3	3.63	13.10	LSPR and better hole collection	[116]
Cu-Au	PTB7-th:PC <sub>61</sub> BM	50	40	HEL	57.9	7.13	9.50	LSPR and better hole collection	[116]
Cu-Au	PTB7-th:PC <sub>71</sub> BM	50	40	HEL	60.1	8.48	12.60	LSPR and better hole collection	[116]

FF: field factor, PCE: power conversion efficiency, HEL: hole extraction layer, (-): no data provided.

to remarkable properties for nanomaterial applications. Poly(ethylene glycol) (PEG)-capped Au NPs with a diameter of ~18 nm were doped into the PEDOT:PSS for OPV [115]. A PCE of 3.51% was obtained at the optimised concentration (0.32 wt%) of PEG-capped Au NPs in PED-OT:PSS with the device structure of ITO/PEG-capped Au NPs:PEDOT:PSS/P3HT:PCBM/LiF/Al. There was a 13% improvement as compared to the bare PEDOT:PSS, possibly because PEG-Au NPs reduce the resistance of the PEDOT:PSS layer. Upon increasing the PEG-capped AuNP concentration, the surface morphology of the PEG-capped Au NP:PEDOT:PSS film also increases in roughness by 5% (0.32 wt%) and 40% (0.64 wt%), respectively. Higher anode surface roughness led to a higher interface area between the anode and the active layer and enhanced the device's hole collection. Performance is achieved with no discernible difference in the transmission of PEDOT:PSS with or without Au NPs, so the performance enhancement was concluded to not be due to the optical effects.

Cu-Au bimetallic NPs with core-shell nanostructures with highly stable and broad LSPR has been reported [116]. In particular, LSPR bands for Au NPs and CuNPs are at 530 nm [117] and 590 nm [118], respectively, while Cu-Au NPs exhibit a wide absorption peak at wavelengths 650–700 nm. The PCEs of the P3HT:PC $_{61}$ BM, PTB7-th: PC $_{61}$ BM, and PTB7-th:PC $_{71}$ BM based organic solar cells were 3.63, 7.13, and 8.48%, respectively. After incorporating 0.88 wt% Cu-Au NPs into the PEDOT:PSS, the improvements are 13.1, 9.5, and 12.6%, respectively. The reason for improvement is the increase in the  $J_{sc}$  or the plasmonic effect from the Cu-Au NPs, IPCE; this is confirmed by the optical absorption measurements [116].

# 4 Outlook and challenges

Overall, the best consistent improvement in efficiency is obtained for devices with metallic NPs doped with PEDOT:PSS for OLEDs (up to 96%) and OPVs (up to 67%), which involve the effects of SPR. OLEDs with the best performance is obtained from the devices with codoped Au NPs and Ag NPs in PEDOT:PSS, where the CE, PE, and EQE are  $35.30 \text{ cd/m}^2$ , 8.20 lm/A, and 9.80%, respectively. The efficiency was improved by 96% with the co-doped NPs, the huge enhancement is mainly attributed to SPR and the synergistic effect from the stronger near-field resonance of Au NPs and the relative broadband resonance of Ag NPs. The co-doped devices showed better electrical properties and long-term stability of OLED devices [73]. For OPV, the most significant improvement of 67% was obtained when Au NPs (14  $\pm$ 4 nm) were doped in PEDOT:PSS. The improvement is due to the SPR effect and better hole collection [98]. On the other hand, the device with co-doped Au and Ag in PEDOT:PSS resulted in PCE of 8.67%, which was improved by 19.6% [102]. The improvement was ascribed to the broad wavelength range of the two distinct metal particles.

In SPR, resonant oscillation of conduction electrons occurs between the negative and positive permittivity materials. LSPR occurs when the incident light matches the frequency of the metallic surface and causes free surface electrons to oscillate collectively, this has been seen in the case of using gold or silver NPs. The schematic of LSPR is illustrated in Figure 7. The enhanced near-field amplitude of these electrons thus occurs at the resonance wavelength. The extinction wavelength and improvement of emission for LSPR are determined by the shape

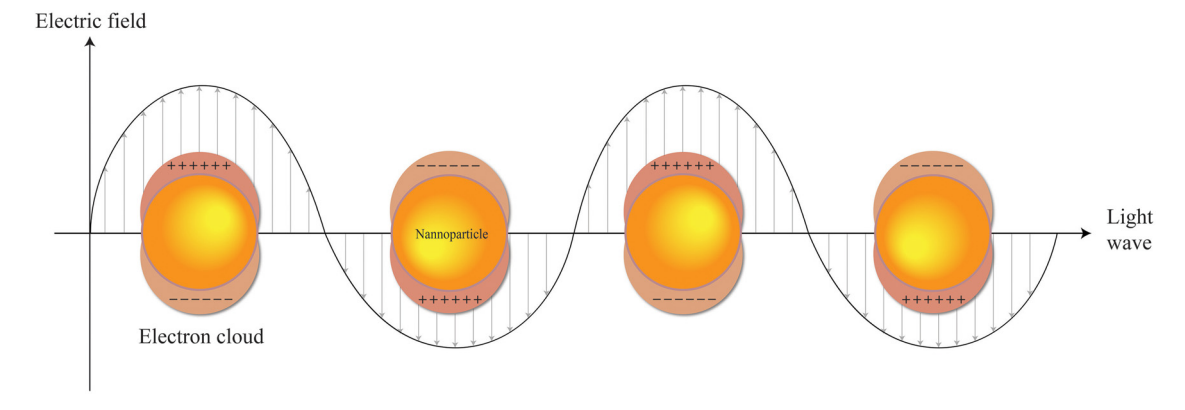


Figure 7: Schematic of LSPR where incident light caused the free conduction electrons in the metal NPs to collective oscillation.

and size of the NPs [1,39]. Different sizes, shapes, and structures of NPs that match the photoluminescence (PL) of the emissive layer will be significantly enhanced [21].

The size of plasmonic NPs that exhibit forward scattering is typically between 30 and 70 nm [119,120] (Figure 8a). As the particle size increases, more light is scattered, thus improving the light-out coupling for OLED devices. However, large NPs embedded in the layer are bad for the device because of the inferior layer morphology and strong metallic absorption [121]. The optimum size of plasmonic NPs for OLEDs is in the region of 50-70 nm to achieve the optimum device efficiency [120]. Furthermore, for plasmonic NPs less than 30 nm, the enhancement is dominantly from the LSPR effect instead of scattering [122]. The plasmonic nearfield induced in the buffer layer (Figure 8b) is able to enhance the absorption and electric field of OPVs [122]. NPs with different shapes and sizes trigger surface plasmonic effects in organic optoelectronic [123-125]. NPs size in the range of 20-60 nm in PEDOT:PSS exhibited a more significant enhancement in OLED devices (30–100%). while minor enhancement was obtained when the size is less than 20 nm. Whereas, in the case of OPVs, smaller NPs (10-20 nm) in PEDOT:PSS is preferable for more extensive PCE enhancement (20-70%). The enhancement is lower when the size is larger than 20 nm.

In addition, metal oxide NPs also show significant enhancement for OLEDs and OPVs. The highest enhancement in current efficiency for OLEDs is 760.5% for the device with  $TiO_2$  NPs (20 wt%, 25 nm) doped PEDOT:PSS

compared to a bare PEDOT:PSS layer [79]. The current efficiency is  $7.30 \text{ cd/m}^2$ , and the power efficiency is 3.15 lm/A. The impressive improvement was achieved due to improved light out-coupling from light scattering from the modified layer. The best enhancement in power conversion efficiency (81%) are obtained for the OPV devices with GO:PEDOT:PSS. GO sheets were first pre-heated and then mixed with the PEDOT:PSS solution. Pre-annealing of GO sheets significantly improves hole collection ability, with 1.8 times improvement over pristine PEDOT:PSS as a buffer layer [114]. The addition of NPs to PEDOT:PSS improves hole injection and conductivity by lowering the sheet resistance of the film after mixing GO with PEDOT:PSS [83]. Films with low sheet resistance, high transparency, and high conductivity are critical for ITO-free OLEDs. Incorporating GO into PEDOT:PSS improves surface morphology and higher work function, which is advantageous for hole injection. The overview effects of NPs:PEDOT:PSS in OLEDs and OPVs are shown in Figure 9.

Although promising results have been obtained with the reviewed strategies for doping NPs in PEDOT:PSS, the quest to find a universal solution to improve the efficiency of OLEDs and OPVs continues. NPs synthesis and the properties of NPs are active research areas with new and rapid development. Thus, there are still a lot of new, possible approaches that are yet to be explored extensively. For example, the size of NPs, shape, and concentrations of NPs are also crucial for OLED and OPV as they affect light out-coupling for OLEDs, light trapping for OPVs, and the electrical properties of the

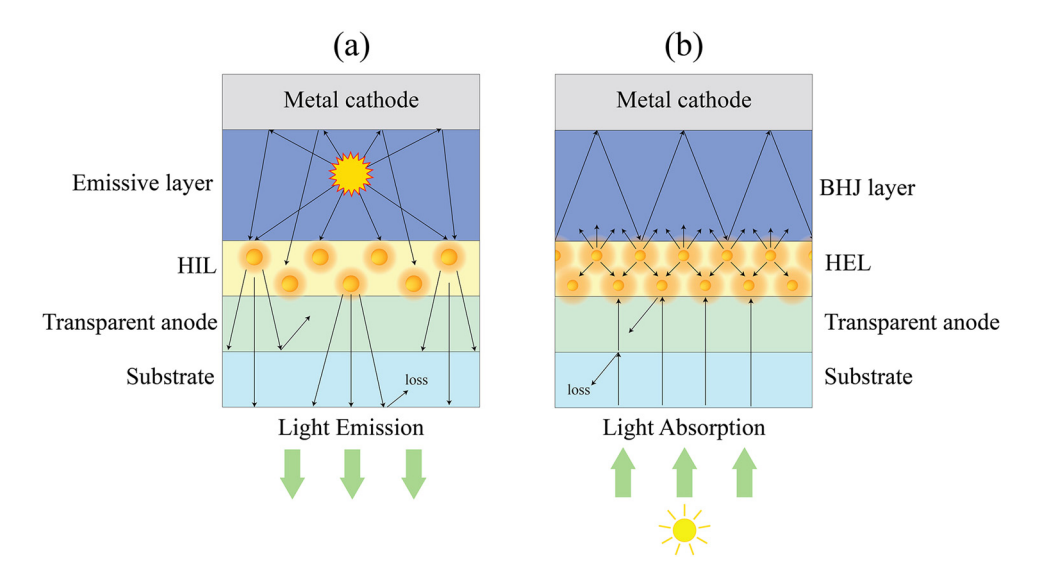


Figure 8: Schematic diagram of OLEDs and OPVs with plasmonic NPs, (a) NPs in HIL for OLEDs with scattering effect and (b) NPs in HEL for OPVs with LSPR effect.

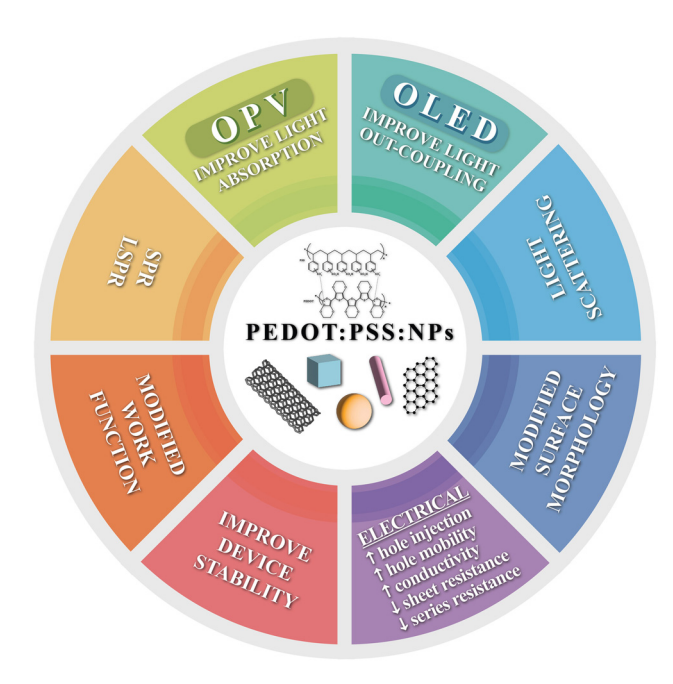


Figure 9: Overview effect of NPs-doped PEDOT:PSS for OLED and OPV.

PEDOT:PSS laver. However, in most of the reports, the NPs used are spherical and rod in shape [21]. To our best knowledge, an extensive study into the effects of particle shape has not been reported in nanoparticles doped PEDOT:PSS for OLEDs and OPVs specifically. Shapedependent metal NPs in the active layer were studied in depth. The various polyhedral gold (Au) NPs are included; cubic, rhombic dodecahedral (RD), edge and corner truncated octahedra (ECTO), and triangular shape are used in the device ITO/ZnO/P3HT:PC<sub>61</sub>BM:NPs/MoO<sub>x</sub>/ Ag [126] (Figure 10). LSPR peaks were detected at 590 nm (cubes and RD), 558 nm (ECTO), and 564 nm (triangular) for each shape. Au NPs with a RD shape have the greatest increase in PCE from 3.4 to 4.4%, followed by ECTO, cube, and triangle (RD > ECTO > cube > triangle). In addition, to further verify the electromagnetic field around the particle surface, 3-dimensional FDTD using transverse electric polarisation with an excitation wavelength of 550 nm was also performed. The result showed that LSPRs around the edges or corners of the RD was significantly enhanced and presented the most potent electric-field responses, followed by ECTO and cube (RD > ETCO > cube). The FDTD results are shown in Figure 11. For Au triangular plates, no electric resonance was induced; thus, the enhancement is mainly caused by scattering. Meanwhile, both simulation and experimental results showed that Au RD NPs demonstrate the most significant enhancement [126].

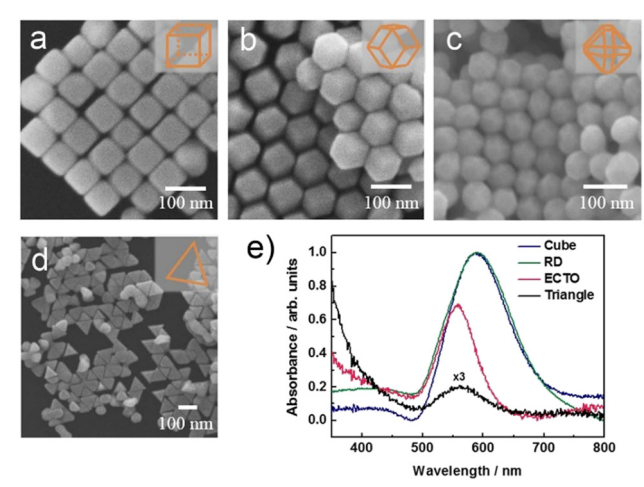


Figure 10: SEM images of: (a) cubes, (b) RD, (c) ECTO, and (d) triangular plates of AuNPs. (e) Absorption spectra of cubes, RD, ECTO, and triangular plates of AuNPs solutions [126]; Copyright (2015) American Chemical Society.

It has also been challenging to study the individual effects of NP doped PEDOT:PSS, such as SPR, scattering, carrier transport, *etc*. The complex optical and electrical processes are difficult to be modelled in numerical simulation alone; thus, extensive experimental work is needed. The combination of both experimental results and numerical analysis can contribute to a better understanding of the carrier behaviour caused by the NP doped PEDOT:PSS layer. On the other hand, non-conducting or non-metallic-based NPs can be used to study pristine optical effects

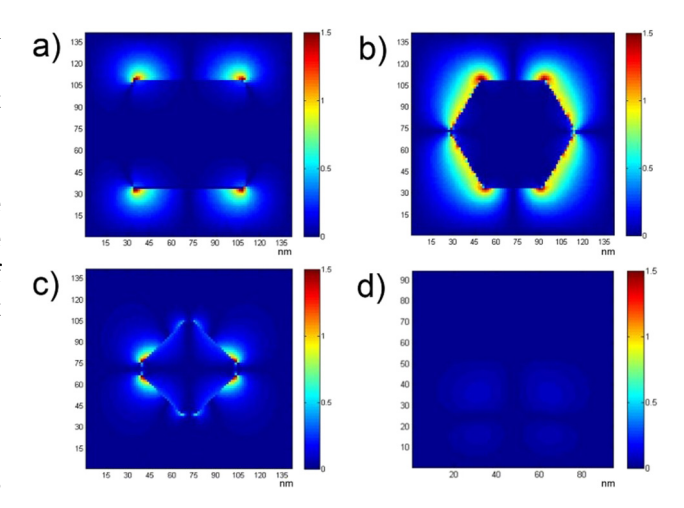


Figure 11: FDTD simulation analysis of time-averaged and normalised transverse electric field distribution with different polyhedral AuNPs: (a) cube, (b) RD, (c) ECTO, and (d) triangle plate. [126]; Copyright (2015) American Chemical Society.

such as scattering, reflectivity, and excluding the plasmonic effect.

Furthermore, ITO-free TCF have recently received much attention because of the scarcity of indium and the process cost. The estimated ITO cost range of organic solar cells is around 40–150 € per m<sup>2</sup>, PET/ITO accounting for the largest share of total costs, around 38-51% of the total cost of the device [127]. Therefore, alternative materials like PEDOT:PSS are able to lower the cost by using the roll-to-roll process. PEDOT:PSS has a higher HOMO level than ITO, making it more suitable for hole injection, but the low conductivity of PEDOT:PSS limits its application. Thus, NPs doped with PEDOT:PSS have also been explored [124]. PEDOT:PSS with AgNW, GO, etc., have been used to improve the conductivity, but the best conductivity is still in the range of 800–1,500 S/cm [128–130]. The performance remains poor and needs to be improved, and the physical mechanism of the composite electrode remains unclear [60].

# 5 Conclusion

Despite advancements, organic optoelectronics continues to face significant challenges in device stability, including degradation, efficient charge transport, light absorption (OPV), and light out-coupling (OLEDs). NPs doped PEDOT:PSS hole transport layer is one of the promising solutions for both devices because of its capability to improve photo absorption or light out-coupling by either increasing the light scattering process or plasmonic resonance effect without increasing the active layer thickness. At the same time, the morphology of the doped PEDOT:PSS layer can also be optimised. Although the optical properties of NPs, such as plasmonic effects, have received the most attention to date, the effects on the electrical properties of organic optoelectronics, such as charge carrier extraction after exciton dissociation, are not entirely understood and remain a major challenge.

This review highlights the recent effort of NP incorporation in PEDOT:PSS for OLEDs and OPVs. It is clear that the presence of NPs in PEDOT:PSS affords a straightforward yet promising solution to increase the light outcoupling from OLEDs and also better light trapping in OPVs. A few typical effects of the NPs enhance the optical and electrical properties. Optical effects include the surface plasmon effect due to NPs, enhanced scattering, and better absorption of photons. In addition, the SPR effects also improved the hole injection, hence electrical conduction by increasing the hole mobility for organic optoelectronics.

Although most of these published works focused on the SPR effects of metallic NPs, other factors that contributed to the device improvement, such as the charge carrier extraction after dissociation and the effects of the shape of the NPs are still not fully understood for plasmonic-based OPVs. In addition, the electrical and morphological properties of the composite are also crucial in nanoscale devices. Further understanding and development will undoubtedly accelerate the implementation of lowcost, large-scale manufacturing.

Funding information: The authors acknowledge the support from the Ministry of Education, Malaysia (FRGS/1/ 2019/STG07/MMU/02/1). S.S. Yap acknowledges the support from the Sandisk/Western Digital Malaysia and the Penang State Government.

Author contributions: All authors have accepted responsibility for the entire content of this manuscript and approved its submission.

Conflict of interest: The authors state no conflict of interest.

# References

- [1] Kim T, Kang H, Jeong S, Kang DJ, Lee C, Lee CH, et al. Au@Polymer core-shell nanoparticles for simultaneously enhancing efficiency and ambient stability of organic optoelectronic devices. ACS Appl Mater Interfaces. 2014;6(19):16956-65.
- [2] Burroughes JH, Bradley DDC, Brown AR, Marks RN, Mackay K, Friend RH, et al. Light-emitting diodes based on conjugated polymers. Nature. 1990;347(6293):539-41.
- Ong GL, Zhang Q, Ong TS, Kek R, Nee CH, Tou TY, et al. [3] Enhanced performance of blue OLED with water/alcohol soluble conjugated polymer as electron injection layer. Synth Met. 2021;272:116658.
- [4] Wu JL, Chen FC, Hsiao YS, Chien FC, Chen P, Kuo CH, et al. Surface plasmonic effects of metallic nanoparticles on the performance of polymer bulk heterojunction solar cells. ACS Nano. 2011;5(2):959-67.
- [5] Cui M, Rui H, Wu X, Sun Z, Qu W, Qin W, et al. Coexistent integer charge transfer and charge transfer complex in F4-TCNQ-doped PTAA for efficient flexible organic light-emitting diodes. J Phys Chem Lett. 2021;12:8533-40.
- [6] Zhang N, Tian G, Wu X, Qin W, Liu M, Li Y, et al. Low driving voltage and enhanced performance of solution-processed blue flexible organic light-emitting diode with PTAA/AgNWs/ PTAA composite hole injection layers. J Phys D Appl Phys. 2019;52(31):8.
- [7] Peng CC, Yang SY, Li HC, Xie GH, Cui LS, Zou SN, et al. Highly efficient thermally activated delayed fluorescence via an

- unconjugated donor-acceptor system realizing EQE of over 30%. Adv Mater. 2020;32(48):1-7.
- [8] Su R, Zhao Y, Yang F, Duan L, Lan J, Bin Z, et al. Triazolotriazine-based thermally activated delayed fluorescence materials for highly efficient fluorescent organic light-emitting diodes (TSF-OLEDs). Sci Bull. 2021;66(5):441-8.
- [9] Fan B, Li M, Zhang D, Zhong W, Ying L, Zeng Z, et al. Tailoring regioisomeric structures of  $\pi$ -conjugated polymers containing monofluorinated  $\pi$ -bridges for highly efficient polymer solar cells. ACS Energy Lett. 2020;5(6):2087-94.
- You YJ, Song CE, Hoang QV, Kang Y, Goo JS, Ko DH, et al. Highly efficient indoor organic photovoltaics with spectrally matched fluorinated phenylene-alkoxybenzothiadiazolebased wide bandgap polymers. Adv Funct Mater. 2019;29(27):1-11.
- [11] Shi M, He Y, Sun Y, Fang D, Miao J, Ali MU, et al. Bis(diphenylamino)-benzo[4,5]thieno[3,2-b]benzofuran as hole transport material for highly efficient RGB organic lightemitting diodes with low efficiency roll-off and long lifetime. Org Electron. 2020;84:105793.
- Nam M, Chung NK, Shim S, Yun JY, Kim JT, Pyo SG. Efficiency [12] enhancement of fluorescence blue organic light-emitting diodes by incorporating Ag nanoparticles layers due to a localized surface plasmon. J Korean Phys Soc. 2017;71(5):299-303.
- [13] Mucur SP, Tumay TA, San SE, Tekin E. Enhancing effects of nanoparticles on polymer-OLED performances. J Nanoparticle Res. 2012;14:10.
- Ong TS, Ong GL, Kee YY, Yap SS, Tou TY. Optimisation of [14] graded-mixed transport organic light emitting diode via mixed-source thermal evaporation technique. Microelectron Eng. 2019;213:62-8.
- [15] Luscombe CK, Maitra U, Walter M, Wiedmer SK. Theoretical background on semiconducting polymers and their applications to OSCs and OLEDs. Chem Teach Int. 2021;3(2):169-83.
- Park CY, Choi B. Enhanced light extraction from bottom emission OLEDs by high refractive index nanoparticle scattering layer. Nanomaterials. 2019;9:9.
- Yamasaki T, Sumioka K, Tsutsui T. Organic light-emitting device with an ordered monolayer of silica microspheres as a scattering medium. Appl Phys Lett. 2000;76(10):1243-5.
- Möller S, Forrest SR. Improved light out-coupling in organic light emitting diodes employing ordered microlens arrays. J Appl Phys. 2002;91(5):3324-7.
- Do YR, Kim YC, Song YW, Lee YH. Enhanced light extraction efficiency from organic light emitting diodes by insertion of a two-dimensional photonic crystal structure. J Appl Phys. 2004;96(12):7629-36.
- Lee MH, Choi WH, Zhu F. Solution-processable organic-inorganic hybrid hole injection layer for high efficiency phosphorescent organic light-emitting diodes. Opt Express. 2016;24(6):A592.
- Zhuang Y, Liu L, Wu X, Tian Y, Zhou X, Xu S, et al. [21] Size and shape effect of gold nanoparticles in "far-field" surface plasmon resonance. Part Part Syst Charact.
- Yang C, Zhao C, Sun Y, Li Q, Islam MR, Liu K, et al. Optical management in organic photovoltaic devices. Carbon Energy. 2021;3(1):4-23.

- Tang Z, Tress W, Inganäs O. Light trapping in thin film organic solar cells. Mater Today. 2014;17(8):389-96.
- [24] Yang Y, Deng H, Fu Q. Recent progress on PEDOT:PSS based polymer blends and composites for flexible electronics and thermoelectric devices. Mater Chem Front. 2020;4(11):3130-52.
- Wen Y, Xu J. Scientific importance of water-processable [25] PEDOT-PSS and preparation, challenge and new application in sensors of its film electrode: a review. J Polym Sci Part A Polym Chem. 2017;55(7):1121-50.
- [26] Woo S, Jeong JH, Lyu HK, Han YS, Kim Y. In situ-prepared composite materials of PEDOT:PSS buffer layer-metal nanoparticles and their application to organic solar cells. Nanoscale Res Lett. 2014:9(1):2-7.
- Lee JH, Kim YY, Park OO. Enhanced performance and [27] mechanical durability of a flexible solar cell from the dry transfer of PEDOT:PSS with polymer nanoparticles. J Mater Chem C. 2018;6(15):4106-13.
- [28] Diker H, Yesil F, Varlikli C. Contribution of O<sub>2</sub> plasma treatment and amine modified GOs on film properties of conductive PEDOT:PSS application in indium tin oxide free solution processed blue OLED. Curr Appl Phys. 2019;19(8):910-6.
- [29] Wageh S, Raïssi M, Berthelot T, Laurent M, Rousseau D, Abusorrah AM, et al. Digital printing of a novel electrode for stable flexible organic solar cells with a power conversion efficiency of 8.5%. Sci Rep. 2021;11(1):1-16.
- [30] Cho EC, Li CP, Huang JH, Lee KC, Huang JH. Three-dimensional conductive nanocomposites based on multiwalled carbon nanotube networks and PEDOT:PSS as a flexible transparent electrode for optoelectronics. ACS Appl Mater Interfaces. 2015;7(21):11668-76.
- Prosa M, Tessarolo M, Bolognesi M, Cramer T, Chen Z, Facchetti A, et al. Efficient and versatile interconnection layer by solvent treatment of PEDOT:PSS interlayer for air-processed organic tandem solar cells. Adv Mater Interfaces. 2016;3(23):1-8.
- [32] Li X, Deng Z, Yin Y, Zhu L, Xu D, Wang Y, et al. Efficiency enhancement of polymer solar cells with Ag nanoparticles incorporated into PEDOT:PSS layer. J Mater Sci Mater Electron. 2014;25(1):140-5.
- Xie Y, Zhang SH, Jiang HY, Zeng H, Wu RM, Chen H, et al. [33] Properties of carbon black-PEDOT composite prepared via in-situ chemical oxidative polymerization. E-Polymers. 2019;19(1):61-9.
- Jonas F, Morrison JT. 3,4-Polyethylenedioxythiophene [34] (PEDT): conductive coatings technical applications and properties. Synth Met. 1997;85(1-3):1397-8.
- [35] Scott JC, Carter SA, Karg S, Angelopoulos M. Polymeric anodes for organic light-emitting diodes. Synth Met. 1997;85(1-3):1197-200.
- Cao Y, Yu G, Zhang C, Menon R, Heeger AJ. Polymer light-[36] emitting diodes with polyethylene dioxythiophene-polystyrene sulfonate as the transparent anode. Synth Met. 1997;87(2):171-4.
- [37] Tian Y, Wang T, Zhu Q, Zhang X, Ethiraj AS, Geng WM, et al. High-performance transparent PEDOT:Pss/CNT films for OLEDs. Nanomaterials. 2021;11:8.
- Hu L, Song J, Yin X, Su Z, Li Z. Research progress on polymer solar cells based on PEDOT:PSS electrodes. Polymers. 2020;12(145):1-19.

- Lim EL, Yap CC, Teridi MA, Teh CH, Jumali MH. A review of recent plasmonic nanoparticles incorporated P3HT:PCBM organic thin film solar cells. Org Electron. 2016;36:12-28.
- [40] Ali AM, Said DA, Khayyat M, Boustimi M, Seoudi R. Improving the efficiency of the organic solar cell (CuPc/C60) via PEDOT:PSS as a photoconductor layer doped by silver nanoparticles. Results Phys. 2020;16:102819.
- Lee W, Kang YH, Lee JY, Jang KS, Cho SY. Improving the thermoelectric power factor of CNT/PEDOT:PSS nanocomposite films by ethylene glycol treatment. RSC Adv. 2016;6(58):53339-44.
- Zhuo MP, Liang F, Shi YL, Hu Y, Wang RB, Chen WF, et al. WO3 nanobelt doped PEDOT:PSS layers for efficient hole-injection in quantum dot light-emitting diodes. J Mater Chem C. 2017;5(47):12343-8.
- [43] Liu J, Li J, Gao C, Chen G. Nanocomposite hole-extraction layers for organic solar cells. Int J Photoenergy. 2011;2011:1-5.
- [44] Wang J, Wang J, Yu H, Yu H, Yu H, Hou C, et al. Solutionprocessable PEDOT:PSS:α-In<sub>2</sub>Se<sub>3</sub> with enhanced conductivity as a hole transport layer for high-performance polymer solar cells. ACS Appl Mater Interfaces. 2020;12(23):26543-54.
- Yang Q, Yu S, Fu P, Yu W, Liu Y, Liu X, et al. Boosting performance of non-fullerene organic solar cells by 2D g-C3N4 doped PEDOT:PSS. Adv Funct Mater. 2020;30(15):2-9.
- Ealias AM, Saravanakumar MP. A review on the classification, characterisation, synthesis of nanoparticles and their application. IOP Conf Ser Mater Sci Eng. 2017;263:3.
- [47] You J, Wang L, Zhao Y, Bao W. A review of amino-functionalized magnetic nanoparticles for water treatment: features and prospects. J Clean Product. 2021;281:124668.
- Singh RP, Handa R, Manchanda G. Nanoparticles in sustainable agriculture: an emerging opportunity. J Control Release. 2021;329:1234-48.
- [49] El-Megharbel SM, Alsawat M, Al-Salmi FA, Hamza RZ. Utilizing of (Zinc oxide nano-spray) for disinfection against "SARS-COV-2" and testing its biological effectiveness on some biochemical parameters during (covid-19 pandemic) -"ZnO nanoparticles have antiviral activity against (SARS-COV-2)". Coatings. 2021;11:4.
- [50] Dasari S, Yedjou CG, Brodell RT, Cruse AR, Tchounwou PB. Therapeutic strategies and potential implications of silver nanoparticles in the management of skin cancer. Nanotechnol Rev. 2020;9(1):1500-21.
- Ye P, Ye Y, Chen X, Zou H, Zhou Y, Zhao X, et al. Ultrasmall Fe<sub>3</sub>O<sub>4</sub> nanoparticles induce S-phase arrest and inhibit cancer cells proliferation. Nanotechnol Rev. 2020;9(1):61-9.
- [52] Zhang DD, Xu JL, Sun HB. Toward high efficiency organic light-emitting diodes: role of nanoparticles. Adv Opt Mater. 2021;9(6):1-19.
- Jaji ND, Lee HL, Hussin MH, Akil HM, Zakaria MR, Othman MBH. [53] Advanced nickel nanoparticles technology: from synthesis to applications. Nanotechnol Rev. 2020;9(1):1456-80.
- Liu Y, Jia M, Song C, Lu S, Wang H, Zhang G, et al. Enhancing [54] ultra-early strength of sulphoaluminate cement-based materials by incorporating graphene oxide. Nanotechnol Rev.
- [55] Du M, Jing H, Gao Y, Su H, Fang H. Carbon nanomaterials enhanced cement-based composites: advances and challenges. Nanotechnol Rev. 2020;9(1):115-35.

- Li X, Wang W, Dong F, Zhang Z, Han L, Luo X, et al. Recent advances in noncontact external-field-assisted photocatalysis: from fundamentals to applications. ACS Catal. 2021;11(8):4739-69.
- [57] Li X, Xiong J, Gao X, Huang J, Feng Z, Chen Z, et al. Recent advances in 3D g-C<sub>3</sub>N<sub>4</sub> composite photocatalysts for photocatalytic water splitting, degradation of pollutants and CO<sub>2</sub> reduction. J Alloys Compd. 2019;802:196-209.
- Banin U, Ben-Shahar Y, Vinokurov K. Hybrid semiconductor-[58] metal nanoparticles: from architecture to function. Chem Mater. 2014;26(1):97-110.
- [59] Sanchez LM, Alvarez VA. Advances in magnetic noble metal/ iron-based oxide hybrid nanoparticles as biomedical devices. Bioengineering. 2019;6:3.
- [60] Chen FC, Wu JL, Lee CL, Hong Y, Kuo CH, Huang MH. Plasmonic-enhanced polymer photovoltaic devices incorporating solution-processable metal nanoparticles. Appl Phys Lett. 2009;95(1):1-4.
- Morfa AJ, Rowlen KL, Reilly TH, Romero MJ, Van De Lagemaat J. Plasmon-enhanced solar energy conversion in organic bulk heterojunction photovoltaics. Appl Phys Lett. 2008;92(1):4-7.
- Chen X, Yang X, Fu W, Xu M, Chen H. Enhanced performance [62] of polymer solar cells with a monolayer of assembled gold nanoparticle films fabricated by Langmuir-Blodgett technique. Mater Sci Eng B Solid-State Mater Adv Technol. 2013;178(1):53-9.
- Heo M, Cho H, Jung JW, Jeong JR, Park S, Kim JY. [63] High-performance organic optoelectronic devices enhanced by surface plasmon resonance. Adv Mater. 2011;23(47):5689-93.
- Lian H, Pan M, Han J, Cheng X, Liang J, Hua W, et al. A MoSe<sub>2</sub> quantum dot modified hole extraction layer enables binary organic solar cells with improved efficiency and stability. J Mater Chem A. 2021;9(30):16500-9.
- [65] Feng J, Sun D, Mei S, Shi W, Mei F, Zhou Y, et al. Plasmonicenhanced organic light-emitting diodes based on a graphene oxide/Au nanoparticles composite hole injection layer. Front Mater. 2018;5:1-8.
- [66] Xiao Y, Yang JP, Cheng PP, Zhu JJ, Xu ZQ, Deng YH, et al. Surface plasmon-enhanced electroluminescence in organic light-emitting diodes incorporating Au nanoparticles. Appl Phys Lett. 2012;100(1):2010-4.
- Pan J, Chen J, Zhao D, Huang Q, Khan Q, Liu X, et al. Surface plasmon-enhanced quantum dot light-emitting diodes by incorporating gold nanoparticles. Opt Express. 2016;24(2):A33.
- [68] Chuang MK, Lin CH, Chen FC. Accumulated plasmonic effects of gold nanoparticle-decorated PEGylated graphene oxides in organic light-emitting diodes. Dye Pigment. 2020;180:
- Du H, Guo Y, Cui D, Li S, Wang W, Liu Y, et al. Solution-[69] processed PEDOT:PSS:GO/AgNWs composite electrode for flexible organic light-emitting diodes. Spectrochim Acta -Part A Mol Biomol Spectrosc. 2021;248:119267.
- [70] Kaçuş H, Aydoğan S, Biber M, Metin ON, Sevim M. The power conversion efficiency optimization of the solar cells by doping of (Au:Ag) nanoparticles into P3HT:PCBM active layer prepared with chlorobenzene and chloroform solvents. Mater Res Express. 2019;6:9.

- [71] Notarianni M, Vernon K, Chou A, Aljada M, Liu J, Motta N. Plasmonic effect of gold nanoparticles in organic solar cells. Sol Energy. 2014;106:23-37.
- Kim JH, Lee JH, Kim TH, Seoul C. Effect of silver nanoparticles [72] in the hole injection layer on the performance of organic light emitting diodes. Mater Res Soc Symp Proc. 2006;936:31-4.
- Jayabharathi J, Abirama Sundari G, Thanikachalam V, Panimozhi S. Enhanced internal quantum efficiency of organic light-emitting diodes: a synergistic effect. J Photochem Photobiol A Chem. 2018;364:577-87.
- Piravadllı Mucur S, Tekin E, San SE, Duygulu Ö, Öztürk HÜ, [74] Utkan G, et al. A novel PLED architecture containing biologically synthesized gold nanoparticles and ultra thin silver laver. Opt Mater. 2015:47:297-303.
- [75] Zhang X, Li W, Ling Z, Zhang Y, Xu J, Wang H, et al. Facile synthesis of solution-processed  $MoS_2$  nanosheets and their application in high-performance ultraviolet organic lightemitting diodes. J Mater Chem C. 2019;7(4):926-36.
- Yuan Y, Zhang X, Li D, Zhang X, Wang L, Lu Z, et al. Tailoring hole injection of sol-gel processed WO<sub>x</sub> and its doping in PEDOT:PSS for efficient ultraviolet organic light-emitting diodes. Phys Chem Chem Phys. 2020;22(23):13214-22.
- Zhang Y, Li W, Xu K, Zheng Q, Xu J, Zhang X, et al. Aqueous [77] solution-processed vanadium oxide for efficient hole injection interfacial layer in organic light-emitting diode. Phys Status Solidi Appl Mater Sci. 2018;215(11):1-6.
- [78] Zhang Y, Li W, Xu K, Kang P, Liu L, Wang L, et al. Sol-gel processed vanadium oxide as efficient hole injection layer in visible and ultraviolet organic light-emitting diodes. Opt Laser Technol. 2019;113:239-45.
- [79] Gupta N, Grover R, Mehta DS, Saxena K. Efficiency enhancement in blue organic light emitting diodes with a composite hole transport layer based on poly(ethylenedioxythiophene):poly(styrenesulfonate) doped with TiO2 nanoparticles. Displays. 2015;39:104-8.
- [80] Gupta N, Grover R, Mehta DS, Saxena K. A simple technique for the fabrication of zinc oxide-PEDOT:PSS nanocomposite thin film for OLED application. Synth Met. 2016;221:261-7.
- Yang P, Yan H, Mao S, Russo R, Johnson J, Saykally R, et al. Controlled growth of ZnO nanowires and their optical properties. Adv Funct Mater. 2002;12(5):323-31.
- [82] Yu L, Shearer C, Shapter J. Recent development of carbon nanotube transparent conductive films. Chem Rev. 2016;116(22):13413-53.
- Liu YF, Feng J, Zhang YF, Cui HF, Yin D, Bi YG, et al. Improved efficiency of indium-tin-oxide-free organic light-emitting devices using PEDOT:PSS/graphene oxide composite anode. Org Electron. 2015;26:81-5.
- [84] Zhou Y, Mei S, Feng J, Sun D, Mei F, Xu J, et al. Effects of PEDOT:PSS:GO composite hole transport layer on the luminescence of perovskite light-emitting diodes. RSC Adv. 202010(44):26381-7.
- Tung VC, Kim J, Cote LJ, Huang J. Sticky interconnect for [85] solution-processed tandem solar cells. J Am Chem Soc. 2011;133(24):9262-5.
- Janghouri M, Mohajerani E, Hosseni H. Improved electrooptical performance of OLEDs using PdCo alloy nanoparticles supported on polypropylenimine dendrimergrafted graphene. J Inorg Organomet Polym Mater. 2018;28(3):783-9.

- Park JW, Ullah MH, Park SS, Ha CS. Organic electroluminescent devices using quantum-size silver nanoparticles. J Mater Sci Mater Electron. 2007;18:393-7.
- [88] Zhang DD, Feng J, Wang H, Liu YF, Chen L, Jin Y, et al. Efficiency enhancement in organic light-emitting devices with a magnetic doped hole-transport layer. IEEE Photonics J. 2011;3(1):26-30.
- [89] Lian H, Tang Z, Guo H, Zhong Z, Wu J, Dong Q, et al. Magnetic nanoparticles/PEDOT:PSS composite hole-injection layer for efficient organic light-emitting diodes. J Mater Chem C. 2018;6(18):4903-11.
- [90] Dong Q, Tai F, Lian H, Zhao B, Zhong Z, Chen Z, et al. Realization of efficient light out-coupling in organic lightemitting diodes with surface carbon-coated magnetic alloy nanoparticles. Nanoscale. 2017;9(8):2875-82.
- [91] Bai S, Guo X, Chen T, Zhang Y, Zhang X, Yang H, et al. Solution processed fabrication of silver nanowire-MXene@PEDOT:PSS flexible transparent electrodes for flexible organic light-emitting diodes. Compos Part A Appl Sci Manuf. 2020;139:106088.
- [92] Alkhalayfeh MA, Aziz AA, Pakhuruddin MZ. An overview of enhanced polymer solar cells with embedded plasmonic nanoparticles. Renew Sustain Energy Rev. 2021;141:110726.
- [93] Rycenga M, Cobley CM, Zeng J, Li W, Moran CH, Zhang Q, et al. Controlling the synthesis and assembly of silver nanostructures for plasmonic applications. Chem Rev. 2011;111(6):3669-712.
- [94] Chen CP, Lee IC, Tsai YY, Huang CL, Chen YC, Huang GW. Efficient organic solar cells based on PTB7/PC71BM blend film with embedded different shapes silver nanoparticles into PEDOT:PSS as hole transporting layers. Org Electron. 2018:62:95-101.
- [95] Singh A, Dev A, Das D, Iver PK. Combined influence of plasmonic metal nanoparticles and dual cathode buffer layers for highly efficient rrP3HT:PCBM-based bulk heterojunction solar cells. J Mater Chem C. 2017;5(26):6578-87.
- [96] Said DA, Ali AM, Khayyat MM, Boustimi M, Loulou M, Seoudi R. A study of the influence of plasmonic resonance of gold nanoparticle doped PEDOT:PSS on the performance of organic solar cells based on CuPc/C60. Heliyon. 2019;5(11):e02675.
- [97] Wanninayake AP, Abu-zahra N. Enhanced morphological and optoelectronic properties of organic solar cells incorporating CuO, ZnO and Au nanoparticles. J Mater Environ Sci. 2020;2508(11):1874-84.
- [98] Mutuma BK, Ranganathan K, Matsoso BJ, Wamwangi D, Coville NJ. Effect of gold nanospheres and nanodots on the performance of PEDOT:PSS solar cells. J Nanosci Nanotechnol. 2018;19(5):2747-54.
- [99] Otieno F, Shumbula NP, Airo M, Mbuso M, Moloto N, Erasmus RM, et al. Improved efficiency of organic solar cells using AuNPs incorporated into PEDOT:PSS buffer layer. AIP Adv. 2017:7:8.
- [100] Matsushima T, Bencheikh F, Komino T, Leyden MR, Sandanayaka ASD, Qin C, et al. High performance from extraordinarily thick organic light-emitting diodes. Nature. 2019;572(7770):502-6.
- [101] Li Q, Wang F, Bai Y, Xu L, Yang Y, Yan L, et al. Decahedralshaped Au nanoparticles as plasmonic centers for high performance polymer solar cells. Org Electron. 2017;43:33-40.

- [102] Lu L, Luo Z, Xu T, Yu L. Cooperative plasmonic effect of Ag and Au nanoparticles on enhancing performance of polymer solar cells. Nano Lett. 2012;13(1):59-64.
- [103] Singh A, Dey A, Iyer PK. Collective effect of hybrid Au-Ag nanoparticles and organic-inorganic cathode interfacial layers for high performance polymer solar cell. Sol Energy. 2018;173(July):429-36.
- [104] Zhang X, Zhang B, Ouyang X, Chen L, Wu H. Polymer solar cells employing water-soluble polypyrrole nanoparticles as dopants of PEDOT:PSS with enhanced efficiency and stability. J Phys Chem C. 2017;121(34):18378–84.
- [105] Liu R. Hybrid organic/inorganic nanocomposites for photovoltaic cells. Materials. 2014;7(4):2747-71.
- [106] Park Y, Müller-Meskamp L, Vandewal K, Leo K. PEDOT:PSS with embedded TiO2 nanoparticles as light trapping electrode for organic photovoltaics. Appl Phys Lett. 2016;108:25.
- [107] Li J, Qin J, Liu X, Ren M, Tong J, Zheng N, et al. Enhanced organic photovoltaic performance through promoting crystallinity of photoactive layer and conductivity of hole-transporting layer by  $V_2O_5$  doped PEDOT:PSS hole-transporting layers. Sol Energy. 2020;211:1102–9.
- [108] Ramasamy MS, Ryu KY, Lim JW, Bibi A, Kwon H, Lee JE, et al. Solution-processed PEDOT:PSS/MoS<sub>2</sub> nanocomposites as efficient hole-transporting layers for organic solar cells. Nanomaterials. 2019;9:9.
- [109] Wang Y, Luo Q, Wu N, Wang Q, Zhu H, Chen L, et al. Solution-processed MoO<sub>3</sub>:PEDOT:PSS hybrid hole transporting layer for inverted polymer solar cells. ACS Appl Mater Interfaces. 2015;7(13):7170-9.
- [110] Zheng Z, Hu Q, Zhang S, Zhang D, Wang J, Xie S, et al. A highly efficient non-fullerene organic solar cell with a fill factor over 0.80 enabled by a fine-tuned hole-transporting layer. Adv Mater. 2018;30(34):1-9.
- [111] Vohra V, Kawashima K, Kakara T, Koganezawa T, Osaka I, Takimiya K, et al. Efficient inverted polymer solar cells employing favourable molecular orientation. Nat Photonics. 2015;9(6):403-8.
- [112] Wang Y, Li N, Cui M, Li Y, Tian X, Xu X, et al. High-performance hole transport layer based on WS<sub>2</sub> doped PEDOT:PSS for organic solar cells. Org Electron. 2021;99:2-6.
- [113] Dehsari HS, Shalamzari EK, Gavgani JN, Taromi FA, Ghanbary S. Efficient preparation of ultralarge graphene oxide using a PEDOT:PSS/GO composite layer as hole transport layer in polymer-based optoelectronic devices. RSC Adv. 2014;4(98):55067-76.
- [114] Yin B, Liu Q, Yang L, Wu X, Liu Z, Hua Y, et al. Buffer layer of PEDOT:PSS/graphene composite for polymer solar cells. J Nanosci Nanotechnol. 2010;10(3):1934–8.
- [115] Fung DDS, Qiao L, Choy WCH, Wang C, Sha WEI, Xie F, et al. Optical and electrical properties of efficiency enhanced polymer solar cells with Au nanoparticles in a PEDOT-PSS layer. J Mater Chem. 2011;21(41):16349-56.
- [116] Tang M, Sun B, Zhou D, Gu Z, Chen K, Guo J, et al. Broad-band plasmonic Cu-Au bimetallic nanoparticles for organic bulk heterojunction solar cells. Org Electron. 2016;38:213.

- [117] Wang DH, Kim DY, Choi KW, Seo JH, Im SH, Park JH, et al. Enhancement of donor – acceptor polymer bulk heterojunction solar cell power conversion efficiencies by addition of Au nanoparticles. Angew Chemie – Int Ed. 2011;50(24):5519–23.
- [118] Yang HJ, He SY, Chen HL, Tuan HY. Monodisperse copper nanocubes: synthesis, self-assembly, and large-area dense-packed films. Chem Mater. 2014;26(5):1785-93.
- [119] Baek SW, Noh J, Lee CH, Kim B, Seo MK, Lee JY. Plasmonic forward scattering effect in organic solar cells: a powerful optical engineering method. Sci Rep. 2013;3:1–7.
- [120] Cho C, Kang H, Baek SW, Kim T, Lee C, Kim BJ, et al. Improved internal quantum efficiency and light-extraction efficiency of organic light-emitting diodes via synergistic doping with Au and Ag nanoparticles. ACS Appl Mater Interfaces. 2016;8(41):27911–9.
- [121] Wu B, Wu X, Guan C, Tai KF, Yeow EKL, Fan HJ, et al.
  Uncovering loss mechanisms in silver nanoparticle-blended
  plasmonic organic solar cells. Nat Commun. 2013;4:1–7.
- [122] Feng L, Niu M, Wen Z, Hao X. Recent advances of plasmonic organic solar cells: photophysical investigations. Polymers. 2018:10(2):1-33.
- [123] Cho H, Shin JW, Cho NS, Moon J, Han JH, Kwon YD, et al. Optical effects of graphene electrodes on organic lightemitting diodes. IEEE J Sel Top Quantum Electron. 2016;22:1.
- [124] Ko SJ, Choi H, Lee W, Kim T, Lee BR, Jung JW, et al. Highly efficient plasmonic organic optoelectronic devices based on a conducting polymer electrode incorporated with silver nanoparticles. Energy Environ Sci. 2013;6(6):1949-55.
- [125] Kalfagiannis N, Karagiannidis PG, Pitsalidis C, Panagiotopoulos NT, Gravalidis C, Kassavetis S, et al. Plasmonic silver nanoparticles for improved organic solar cells. Sol Energy Mater Sol Cells. 2012;104:165–74.
- [126] Tseng WH, Chiu CY, Chou SW, Chen HC, Tsai ML, Kuo YC, et al. Shape-dependent light harvesting of 3D gold nanocrystals on bulk heterojunction solar cells: plasmonic or optical scattering effect? J Phys Chem C. 2015;119(14):7554-64.
- [127] Machui F, Hösel M, Li N, Spyropoulos GD, Ameri T, Søndergaard RR, et al. Cost analysis of roll-to-roll fabricated ITO free single and tandem organic solar modules based on data from manufacture. Energy Environ Sci. 2014;7(9):2792–802.
- [128] Wu X, Liu J, Wu D, Zhao Y, Shi X, Wang J, et al. Highly conductive and uniform graphene oxide modified PEDOT:PSS electrodes for ITO-Free organic light emitting diodes. J Mater Chem C. 2014;2(20):4044–50.
- [129] Kim S, Kim SY, Chung MH, Kim J, Kim JH. A one-step roll-toroll process of stable AgNW/PEDOT:PSS solution using imidazole as a mild base for highly conductive and transparent films: optimizations and mechanisms. J Mater Chem C. 2015;3(22):5859-68.
- [130] Das Neves MFF, Damasceno JPV, Holakoei S, Rocco MLM, Zarbin AJG, De Oliveira CKBQM, et al. Enhancement of conductivity and transmittance of graphene oxide/PEDOT:PSS electrodes and the evaluation of charge transfer dynamics. J Appl Phys. 2019;126:21.